NATIONAL ADVISORY COMMITTEE FOR AERONAUTICS

TECHNICAL MEMORANDUM

No. 1131

GAS-DYNAMIC INVESTIGATIONS OF THE PULSE-JET TUBE

PARTS I AND II

By F. Shultz-Grunow

Technical High School
Aachen, Germany

Washington
February 1947

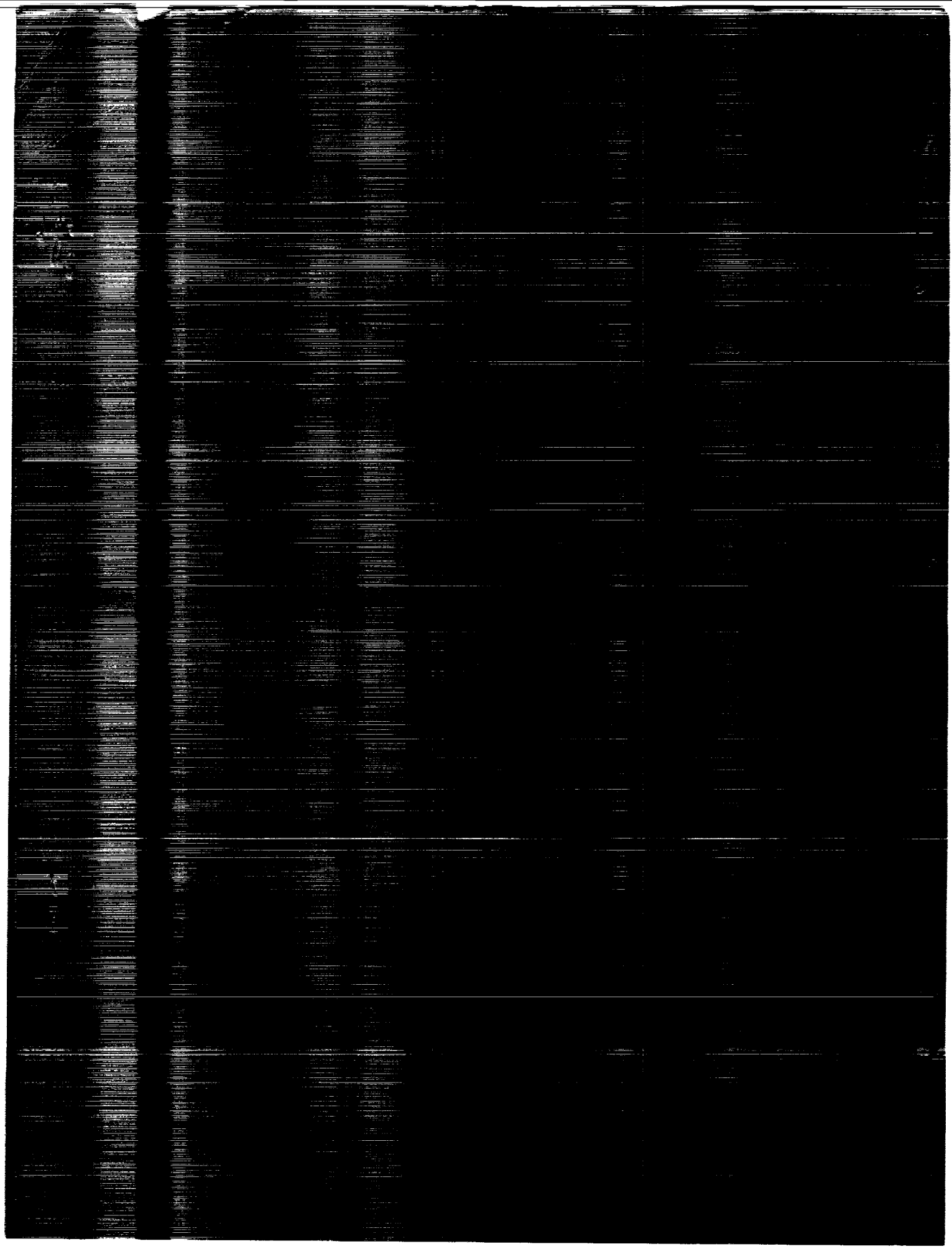

FOREWORD

The gas-dynamic investigations of the pulse-jet tube conducted at the Technical High School at Aachen is presented in two parts. Part I was issued in June 1943 and Part II in August 1944; both parts are presented here under one cover. The contents of each part is shown by the following brief summaries:

Part I - Influence of the form of the jet tube, of the effective cross-sectional area of the valves, of leakiness in the valves, and of the speed of flight on the mode of operation of the pulse-jet tube and on the ratio of the amount of charge induced for the second cycle to the standard charge postulated for the first cycle.

Part II - Consideration of the sequence of pressure changes during combustion.

NATIONAL ADVISORY COMMITTEE FOR AERONAUTICS

TECHNICAL MEMORANDUM NO. 1131

GAS-DYNAMIC INVESTIGATIONS OF THE PULSE-JET TUBE*

PART I

By F. Schultz-Grunow

SUMMARY

Based upon a simplified representation of the mode of operation of the pulse-jet tube, the effect of the influences mentioned in the title were investigated and it will be shown that, for a jet tube with a form designed to be aerodynamically favorable, the ability to operate is at least questionable.

INTRODUCTION

The jet tube discussed herein is shown in its simplest cylindrical form in figure 1. Distributed over the cross section at the left-hand or inlet end of the tube are air valves that open automatically whenever the pressure within the tube is lower than that outside and permit only inward flow. Here also are located fuel-injection valves, which likewise open automatically at low pressure within the tube. The right-hand, or exhaust, end of the tube is open.

In a correctly proportioned jet tube, if a fuel-air mixture initially present in the inlet end of the tube in sufficient quantity is ignited, an automatically repeating working cycle begins, which consists of the explosion of the fresh charge, its exhaust, the sucking in behind it of a new mixture by the inertia of the exhausting gas column, and the automatic ignition of the new mixture, wherewith the process begins anew. The fuel-energy introduced is so transformed into heat and kinetic energy that exhaust occurs at a greater velocity than that of intake, whence a thrust results.

---

*"Gasdynamische Untersuchungen am Verpuffungstrahlrohr." Inst. f. Mech., Tech. Hochschule Aachen (ZWB), Forschungsbericht Nr. 2015/1 u. 2.

In particular, the processes of nonuniform movement in the tube will be discussed here on the basis of the law of propagation of gas-pressure waves of finite amplitude and in the simplest manner, namely, assuming adiabatic changes of state and further assuming that at the beginning of the working cycle there is present, adiabatically compressed relative to the surrounding air, a column of fresh charge, which suddenly expands. In accordance with the data given by Paul Schmidt, let the length of the column of fresh charge be one-seventh of the tube length, and the initial pressure 1.5 atmospheres above local atmospheric pressure.

These prescribed initial conditions largely predetermine the temporal course of variation of the excess pressure at the inlet cross section of the tube, from which the thrust results. The reader should therefore not expect to find in the following remarks a theoretical method of calculating the thrust; nor could this be expected in any case because the combustion process so completely eludes theoretical treatment that here experimentation alone is decisive. But what can be accomplished is the investigation of all the processes set in motion by the reverberating gas waves and the influence thereon of any structural alterations, combustion pressure, and flight speed. The criterion on which the effect of these factors will be more or less favorably adjusted will be, aside from the ability of the tube to operate, the increase achieved in the quantity of fresh charge sucked in and available at the end of a working cycle, inasmuch as a larger quantity will categorically possess a greater content of thermodynamically useful work. Data so obtained have been confirmed in experiments and have proven useful in the development of a jet-tube form of low air resistance. Moreover, such data facilitate the explanation of many phenomena observed in jet-tube work.

SYMBOLS

x distance, from inlet end toward exhaust end

t time, from beginning of a working cycle

R tube length

R' length of column of fresh charge at beginning of first working cycle

R'' length of column of fresh charge at beginning of second working cycle

u gas velocity

a velocity of sound

a_1 velocity of sound in local atmosphere

a_s velocity of sound at $u = 0$ or at stagnation point

$\xi = x/R$, nondimensional distance

$\tau = ta_1/R$, nondimensional time

$\xi' = R'/R$

$\xi'' = R''/R$

T period of one working cycle

p pressure

p_1 local atmospheric pressure

ρ density

ρ_1 atmospheric density

$\kappa = c_p/c_v = 1.4$

M' quantity of fresh charge at beginning of first working cycle

M'' quantity of fresh charge at beginning of second working cycle

F_R cross-sectional area of tube

F_E total effective cross-sectional area of air valves open for intake

$z = F_E/F_R$

FUNDAMENTALS

Method of investigation.

Making the assumption of one-dimensional movement along the axis of the tube, the pressure waves can be followed graphically in a system of coordinates of which the ordinate is time t and the

abscissa the distance x traveled by the wave. An example of this representation of distance as a function of time is the graphic representation of a railway timetable in figure 2. The train leaves station A at time $t = 0$ and moves toward B with the constant speed u_1. At B it halts for Δt seconds and then proceeds further with the reduced speed u_2. The course of the line in figure 2 shows where the train is at a given time and when it will reach a given place. Its slope as measured from the t-axis represents the speed because $u = \frac{dx}{dt}$. The greater the deviation, the greater the speed. Zero slope from the t-axis indicates a state of rest; a leftward slope would indicate motion in the reverse direction.

In order to understand better the graphic methods to be used herein, reference may here be made to four reports in which the laws of propagation and reflection of pressure waves of finite amplitude in gases were investigated. (See reference 1, p. 322, and references 2 to 4.) According to these reports, there exists in a tube of uniform cross section the following relation between the velocity of sound a and the gas velocity u in an

$$\text{outflowing } (+x \text{ direction}) \text{ wave, } du = -\frac{2}{\kappa - 1} da$$

$$\text{inflowing } (-x \text{ direction}) \text{ wave, } du = +\frac{2}{\kappa - 1} da$$

or integrated

$$\Delta u = \mp \frac{2}{\kappa - 1} \Delta a_i \tag{1}$$

These are linear relations, which permit a and u to be superimposed when opposing waves interact. These relations can also be so arranged that, with reference to the quantities defined by Riemann,

$$r = \frac{1}{2}\left(\frac{2}{\kappa - 1} a + u\right) \quad \text{and} \quad s = \frac{1}{2}\left(\frac{2}{\kappa - 1} a - u\right) \tag{2}$$

there belongs to each element of an outflowing wave an r value that does not change even when an inflowing wave is encountered, and to each inflowing element an s value that likewise does not change. One may further deduce that an outflowing-wave element does not influence the value of s along its path, nor an inflowing-wave element the value of r along its path, so if no encounter takes place, an outflowing wave has a constant s value and an inflowing wave a constant r value.

In the method to be employed, a pressure wave is approximated by a step-curve, as illustrated in figure 3. At each step, which shall hereinafter be designated a wave, a change occurs in the velocity of sound Δa and a change in the gas velocity Δu. If these changes in an outflowing wave are positive, there is a condensation wave; in the opposite case, a rarefaction wave. In order to distinguish them, condensation waves will be shown by solid lines and rarefaction waves by dashed lines. Figure 3 shows the wave propagation in the plane t,x and the whole wave as approximated by the wave elements at various times. The wave is understood to be caused by a variation of pressure operating at $x = 0$. In the diagram, the wave has been divided into equal increments Δu and Δa for the sake of simplicity, namely, $\Delta u = 1.1\ a_1$ and, consequently, from equation (1) with $\kappa = 1.4$, $\Delta a = 0.2\ a_1$. The arrows show the direction of the gas velocity u at each moment. The path of a gas particle in a t,x diagram is always shown as a finely dotted line; the deviation of this line from the t-axis represents u. The path shown is that of a gas particle that is at $x = 0$ when $t = 0$.

The movement and gas conditions in a wave are determined by a and u because pressure and density may be obtained from the adiabatic relations

$$\frac{p}{p_1} = \left(\frac{a}{a_1}\right)^{\frac{2\kappa}{\kappa-1}} \quad \text{and} \quad \frac{\rho}{\rho_1} = \left(\frac{a}{a_1}\right)^{\frac{2}{\kappa-1}} \tag{3}$$

The subscript 1 always indicates the atmospheric condition in which the jet tube is operating. [NACA comment: The author was able to neglect the differences in temperature between the working fluid and the outside atmosphere because of the dimensionless representation. The calculations were therefore made assuming that the working fluid in a state of rest has the same temperature as the outside atmosphere.]

The velocity of propagation of a wave w is composed of the velocity of sound a and the velocity of the gas u in which it travels. It is [NACA comment: In the general case, this relation is $w = u \pm a$.]

$$w = a + u \tag{4}$$

For the wave marked I in figure 3, $w = a_1 + 2\Delta a + 2\Delta u$ and specifically, as has been said, this velocity is represented in the plane t,x by $\tan \alpha$ (fig. 3). In drawing the wave plan, this slope is

taken from a slope plan shown, on the scale of which the velocity corresponding to a given slope is indicated, both for the positive and, when required, for the negative direction of propagation.

Similarity.

In order to be bound as little as possible to concrete numerical values, the dimensionless coordinates ξ and τ will be used in place of x and t, so

$$\xi = \frac{x}{R} \quad \text{and} \quad \tau = \frac{a_1 t}{R} \tag{5}$$

where R is the tube length. The slope of a propagation line as measured from the τ-axis is then the velocity made dimensionless by dividing by a_1. This mode of representation has the advantage that it is independent of a specific tube length or atmospheric condition (altitude). As a parameter expressing relative lengths, we now have simply

$$\xi' = \frac{R'}{R}$$

(R' = length of compressed column of fresh charge; R = tube length)

The initial pressure of the column of fresh charge, of course, constitutes a further parameter. Because this pressure has not yet been measured, as already stated, take as a reasonable assumption that it is 2.5 times as great as the pressure of the surrounding atmosphere. Then the velocity of sound in the compressed column of fresh charge according to equation (3) is [NACA comment: The ratio a/a_1 of 1.144 has apparently been chosen for convenience in subdivision into wave elements. It actually corresponds to a pressure ratio p/p_1 of 2.565, rather than 2.5.]

$$a = 1.144\ a_1$$

As also mentioned,

$$\xi' = \frac{R}{R'} = \frac{1}{7}$$

is taken as the normal case.

The absolute length of the tube does not appear here as a parameter, which is contrary to practical experience, because frictional and heat losses are disregarded.

As the final parameter, z is obtained, the ratio of the intake cross section F_E (effective flow area of the valves) to the tube cross section F_R

$$z = \frac{F_E}{F_R}$$

In using parameters, it is assumed that two tubes will behave similarly if all their parameter values are the same.

BOUNDARY CONDITIONS IN THE JET TUBE FOR WAVE REFLECTION

Wave reflection at the closed and at the open end of the tube, as well as at abrupt changes of cross section (a series that is considered as the approximate equivalent of a gradual change of cross section) have been previously treated (references 3 and 4).

Closed end of tube.

At the closed end of the tube, the gas velocity is always zero, whence it follows that a wave will be reflected with the same strength and with the same sign as in acoustics.

Open end of tube.

The pressure that exists at the open end of the tube during outward flow is that of the surrounding atmosphere, because the discharge is in the form of a jet; during inward flow there exists a sink flow and consequently a Bernoulli pressure decrease, which is determined by the Bernoulli equation

$$\frac{a^2}{\kappa - 1} + \frac{u^2}{2} = \frac{a_1^2}{\kappa - 1}$$

in which pressure is expressed by sound velocity. From this it follows, that so long as outflow exists, a wave will be reflected at full strength with opposite sign; but not so in the case of inflow, as a part of the wave then creates the Bernoulli pressure drop. With a decrease in the inflow, the Bernoulli pressure drop diminishes. This need not be further discussed because under the conditions assumed, so small a degree of inflow occurs at the open end of the tube that this pressure drop may be ignored.

Change in cross section.

At a change in cross section, the same quantity of fluid must enter at side A as that which leaves from side B.

$$\rho_A u_A F_A = \rho_B u_B F_B$$

The same applies to the energy:

$$\frac{u_A^2}{2} + \frac{a_A^2}{\kappa - 1} = \frac{u_B^2}{2} + \frac{a_B^2}{\kappa - 1} = \frac{a_s^2}{2} \tag{6}$$

These two conditions, which must apply to the passage of a wave through a change in cross section, may be most simply treated with the aid of a diagram, the so-called characteristics diagram, in which the gas velocity u is taken as the abscissa and the velocity of sound a as the ordinate. The diagram is preferably made dimensionless by dividing by a_1. Individual lines r = constant and s = constant, which from equation (2) are straight lines, are entered in the diagram. These are the characteristics, because at these lines discontinuities may occur, which in the present case are the waves. Actually, a value of r refers to an outflowing wave and a value of s to an inflowing wave. Also in the diagram (fig. 4) are curves of constant energy, which according to equation (6) are ellipses, and curves of constant mass velocity, which are hyperbolas in accordance with the equation

$$\frac{\rho u}{\rho_1 a_1} = \left(\frac{a}{a_1}\right)^{\frac{2}{\kappa-1}} \cdot \frac{u}{a_1} = \text{constant} \tag{7}$$

The passage of a condensation wave through a point of increase of cross section shall be observed, momentary states of which process before and after the reflection are shown in figure 5. The wave brings with it the gas state 6, namely, a_6 and u_6. It traverses state 2, defined by a_2 and u_2. At the point of increase of cross section, there occurs an increase of pressure to state 3. At the interaction of the wave with the tube enlargement, there arises from the wave 6 a wave 4, which proceeds forward, and a reflected wave 5. The states 6 and 5 are separated, according to figure 5, by an inward-traveling rarefaction wave and thus lie on a r = constant line in the a,u diagram; the states 4 and 3 are separated by an outward-traveling condensation wave and thus lie on a s = constant line. States 6 and 3 are known and hence also the r- and s-lines on which states 5 and 4, respectively, lie. States 5 and 4 are separated by the point of change of cross section and thus lie also upon an ellipse. Furthermore there exists between 5 and 4 a difference of mass velocity $\Delta(\rho u)$ determined by the difference in cross section ΔF in accordance with

$$\Delta(\rho u) = \rho_5 u_5 - \rho_4 u_4$$

and

$$\rho_5 u_5 F_5 = \rho_4 u_4 F_4$$

in which F is the cross-sectional area. Hence

$$\Delta(\rho u) = \rho_5 u_5 \frac{\Delta F}{F_4} \tag{8}$$

Thus there is only one ellipse on which 5 and 4 may lie, namely, the one whose points of intersection with the given r- and s-lines have the prescribed difference of mass velocity. The ellipse must be found by trial. In figure 6 the reflection is shown in a t,x diagram. The wave reflected is a rarefaction wave because d_a $a_6 > a_5$ and $u_5 > u_6$. In the case of a reduction in cross section, the reflected wave is a condensation wave.

Reflection at the valves.

The valves at the intake end behave like a solid wall, so long as there is an excess of pressure against their inner sides. But when the pressure is less than that outside they are open; in this case reflection occurs as at a partly open tube end. Inasmuch as the valves are spring-operated, their openings increase with decreasing inside pressure to a maximum area F_E determined by their mechanical construction. For the sake of simplicity, this spring action shall be disregarded and it shall be assumed that whenever the inside pressure is less than that outside, the valves are fully open. Let F_E be the effective cross-sectional area of the openings, in which the effect of friction and the vena-contracta loss have already been allowed for. The Bernoulli equation (equation (6)) for uniform flow may be applied to the flow through the valves on account of their short flow length. The flow conditions in the valves thus lie in the a,u diagram along an ellipse that intersects the a-axis (that is, the line $u = 0$) at a point corresponding to the value of the sonic velocity at the stagnation point a_s, provided that by a means of suitable fairing (total head scoop) ahead of all the valves, the impact pressure corresponding to the speed of flight is made to operate against their outer sides. Let the state of the gas and condition of motion occurring at the narrowest valve cross section be denoted by 4. Neglecting the shock loss, it is assumed that on the outflow side of the valves, that is, the inner side, there is a uniform distribution of velocity over the tube cross section F_R, and hence

$$\rho_4 u_4 F_4 = \rho_3 u_3 F_3$$

and

$$\Delta(\rho u) = \rho_4 u_4 - \rho_3 u_3 = \rho_4 u_4 \left(1 - \frac{F_E}{F_R}\right) \qquad (9)$$

in which 3 denotes the state of the gas and condition of motion in the tube immediately next to the valves. Because, with the construction chosen, the outflow from the valves occurs without any regaining of pressure, $a_3 = a_4$, and states 3 and 4 lie on a horizontal line in the a,u diagram. For any mass velocity $\rho_4 u_4$, the mass velocity difference $\Delta(\rho u)$ may be computed from equation (9) because F_E/F_R is given by the dimensions of the tube.

Now if a gas and motion condition 1 exists at the discharge side of the valves, through which a rarefaction wave travels bringing with it condition 2 (fig. 7), then a wave will be reflected at the valves that will produce state 3 at the discharge side and state 4 in the narrowest valve cross section. States 1 and 2, because they are separated by an inward-traveling wave, lie on a r = constant line in the a,u diagram (fig. 8); states 2 and 3, being separated by an outward-traveling wave, lie on a s = constant line. The required conditions 3 and 4 lie on that horizontal straight line on which 3 and 4 will have the mass velocity difference $\Delta(\rho u)$ prescribed by equation (9). In figure 8 may be seen four possible cases of the reflection, according to the magnitudes of $\Delta(\rho u)$ and F_E/F_R. At a ratio F_E/F_R in the neighborhood of unity, to which the states 3^1 and 4^1 in figure 8 correspond, a condensation wave will be reflected. Then there is a smaller F_E/F_R value at which no wave will be reflected, states 3^2 and 2 coinciding. At a still smaller F_E/F_R value, a rarefaction wave will be reflected, because 3^3 has smaller state values than 2. At a still smaller F_E/F_R value, there occurs the limiting case in which u = a in the valve cross section (the flow velocity u equals the velocity of sound a); this is condition 4^4. The corresponding state 3^4 is the point of intersection of the s = constant line through 2 with that hyperbola which has the required increment of mass velocity $\Delta(\rho u)$ relative to the hyperbola that passes through 4^4 and is tangent to the ellipse. In figure 9 the reflection in the third case is shown in a t,x diagram.

MODE OF OPERATION OF THE JET TUBE AT REST

Cylindrical Tube

The mode of operation of the cylindrical tube is evident from the wave diagrams in figures 10 and 11, which are drawn for $F_E/F_R = 0.2$ and 0.4, respectively. A part of the excess pressure

of the column of fresh charge travels toward the right as the condensation shock wave a, which is so small that the change of state in it may be regarded as adiabatic. The other part travels leftward as a rarefaction wave; the initial difference of velocities of sound $\Delta a = a - a_1 = 0.144a_1$ (see p. 6) distributes itself one-half to each of the two waves. The rarefaction wave is shown as divided into two elementary waves b and c, in order to allow for the lesser velocity of propagation of later wave elements than that of earlier ones. A further subdivision proves to be unnecessary. The rarefaction wave is reflected at the left end of the tube as from a solid wall because the valves are closed. Finally, therefore shock a and the two waves b and c are traveling toward the right. The states of the gas and conditions of motion created by the shock and the waves are enumerated by the figures in circles, for which the state values, namely, velocity of sound a/a_1 and gas velocity u/a_1, may be found in table I. Positive gas velocity signifies velocity directed toward the right. It may be seen from the table that behind the last rarefaction wave traveling to the right, atmospheric conditions are again attained.

At the right-hand or open end of the tube, the shock is reflected as a rarefaction wave, which is likewise divided into two elementary waves d and e. The rarefaction waves are here reflected at the open end as condensation waves, which soon combine themselves into the shock h.

The rarefaction wave d creates condition 12, for which table I shows pressure lower than the outside atmosphere. As soon as this state reaches the left-hand end of the tube, the valves open and at the moment τ_A fresh charge begins to flow in. Consequently, the finely dotted line representing propagation of the boundary of the fresh charge begins here. The intake process is strengthened by the subsequent rarefaction wave e.

Because of the shock h, which now arrives, the fresh-charge front is forced not merely to stop but to reverse its motion, whereby the fresh charge is compressed. As soon as the shock strikes the valves, the intake period is ended and we have at this moment τ_E a compressed column of fresh charge of the length ξ'' in the tube. It is assumed that at the moment τ_E the explosion of the column of fresh charge occurs, so the length ξ'' then attained has the same significance for the second working cycle as ξ' for the first. Because it turns out that $\xi'' < \xi'$, it must be concluded that the jet tube could only operate if $F_E/F_R > 0.4$. The explanation of the fact that in reality it operates even when $F_E/F_R = 0.2$ lies in

the choice of prescribed conditions. In spite of this inconsistence with reality, figures 10 and 11 show a number of noteworthy particulars that do correspond to reality.

1. The intake process is set in motion by the rarefaction waves d and e into which the condensation shock wave a is transformed without loss of strength by its reflection at the right-hand end of the tube.

2. It appears that the condensation shock wave h, into which the rarefaction waves b and c are transformed by reflection at the right-hand end of the tube, plays a part in the ignition of the fresh charge.

3. At small F_E/F_R ratios of the order of magnitude of 0.3 or less, the rarefaction waves d and e, which start the intake process, are reflected as the waves i and k of the same kind and, in fact, produce a gas velocity directed toward the left so the working cycle ends with an inflow at the exhaust end. In actual fact there has been observed with the Argus tube an inflow at the exhaust end preceding the exhaust of the next cycle when $F_E/F_R = 0.3$.

At $F_E/F_R = 0.4$, waves i and k no longer set in motion a negative velocity; only k is a rarefaction wave. It is thus to be expected that, in agreement with the cited observation, at $F_E/F_R > 0.4$ this inflow at the exhaust end does not occur.

EFFECTS OF CONSTRUCTIONAL ALTERATIONS

Jet Tube at Rest

Influence of length ξ', tube length remaining the same.

The greater ξ', the longer is the path of the rarefaction waves b and c (figs. 10 and 11), so much later is the shock h formed from them and so much longer is the intake period $\tau_E - \tau_A$ and the duration of the working cycle.

The effect on the duration of the working cycle is negligible, amounting to 5 percent. The increased intake period results in an increased quantity of fresh charge M'' at the end of the working cycle. With an increase of ξ' from 0.1145 to 0.191, that is, an increase of 66 percent, there is obtained

F_E/F_R	Increase of M" (percent)
0.4	20
.6	30
.8	30

Influence of tube length R, absolute length of R' remaining the same.

In the limiting case of very weak waves, one would expect, according to the laws of acoustics, an increase in the duration of the working cycle proportional to R. In this case it slowly increases as much as 5 percent because as R increases the rarefaction waves b and c shift nearer to the shock a, thereby reducing the extent of the regions through which the waves d and e move more slowly.

M" increases with increasing R as follows:

F_E/F_R	R/R'	M"
0.4	5.25	0.6
	7	.7
	8.75	.8
0.6	5.25	0.9
	7	.9
	8.75	1.0
0.8	5.25	1.0
	7	1.0
	8.75	1.1

According to this table, the results of lengthening the tube are favorable; of course there is, for reasons not here discussed (heat leakage) a practical limit of about R = 3.5 meters.

Influence of change in valve cross section F_E.

Figure 12 shows the increase of M" with increasing F_E/F_R on the basis of figures 10 and 11 and similar figures.

Influence of tube shape (tube of varying cross section).

The values $\xi' = 1/7$ and $F_E/F_R = 0.4$ were taken as a basis. The tube forms investigated with discontinuous change of cross section, in which each change from left to right always amounts to 50 percent

of the preceding section, are shown in figure 13. Beside them to the right are given the tube forms with continuous change of cross section, to which the investigated stepped forms may be regarded as approximating. Less accurately than before, a rarefaction wave is now represented with one instead of two rarefaction lines, for at each change of cross section each wave gives rise to two, whereby the investigation becomes very complicated.

Form A corresponds to the tube already investigated in figure 11, which is to serve as a basis for comparison.

(a) Reduction of cross section at ξ' (form B):

The fresh-charge front is assumed to lie a little to the left of the constriction. This form corresponds approximately to the cylindrical Argus tube with enlarged combustion chamber.

The applicable wave diagram is given in figure 14. As a result of the constriction, the condensation shock wave a is stronger and the rarefaction wave b is weaker than with form A (fig. 11). Consequently, the rarefaction wave e resulting from the reflection of a is stronger than the corresponding wave in figure 11. The result is smaller velocities of propagation for the subsequent condensation waves f and g and consequently a substantially longer intake period $\tau_E - \tau_A$ than in the case of form A, a substantially larger column of fresh charge being thus drawn in.

In this connection it must be remembered that the returning waves e, f, and g are weakened at the point of change of cross section. The fresh charge will therefore be sucked in with a weaker vacuum than in the case of figure 11. But if the quantity M" newly drawn in is compared, it is found that nevertheless

$$\frac{M''_B}{M''_A} = \frac{0.823}{0.51} = 1.6$$

that is, in spite of the weaker suction the intake period is sufficiently lengthened that form B yields a 60-percent increase in charge.

Through the weakening of the subsequent wave of condensation, the ignition of the new column of fresh charge is made doubtful. Of course, the condensation shock wave creates a higher absolute pressure than in form A. It shall not be attempted to decide which is more decisive for ignition, the absolute pressure or the pressure ratio.

The optimal constriction is that at which the exhaust occurs with a velocity equal to that of sound in the surrounding atmosphere.

(b) Reduction of cross section at center of tube length (form C):

In figure 15 waves d and e, reflected at the constriction, cross the returning waves f and g too late to produce as long an intake period $\tau_E - \tau_A$ as in figure 14. Besides this, there occurs a still smaller pressure drop across the valves, so now

$$\frac{M''_C}{M''_A} = \frac{0.71}{0.51} = 1.39$$

the improvement over form A still amounts to 39 percent.

The pressure ratio in the condensation shock wave h, which produces the ignition, is just a little smaller than with form B; however, the absolute value of the compressing pressure is greater.

(c) Reduction of cross section at exhaust end (form D):

From figures 10 and 11 it may be seen that the automatic operation of the jet tube is based on the circumstance that at the open end a condensation wave is reflected as a rarefaction wave, and a rarefaction wave as a condensation wave, namely, at full strength because at the exhaust end only outflow takes place. Consequently, the first to strike the valves is the rarefaction wave, which starts the intake period, after which the igniting condensation shock wave h reaches them.

But if now the reduction of cross section is located at the exhaust end, this means that there is a half-open tube end at which, as closer investigation shows (fig. 8), the condensation wave is reflected as such with lessened strength and likewise the rarefaction wave is reflected as such with lessened strength. In this case, as shown in figure 16, the condensation and rarefaction waves strike the valves in reversed sequence and the tube does not function.

(d) Two reductions of cross section (form E):

Here the lengthening of the intake period determined for forms B and C is effected by two constrictions of 50 percent each. A longer intake period $\tau_E - \tau_A$ but a lesser intake-producing pressure difference is thus obtained (fig. 17). Likewise, the pressure ratio in the igniting condensation shock wave h is the smallest of those for all tube forms. In practice the absolute compression pressure is of equal magnitude to that obtained with form C. The newly induced quantity of fresh charge M''_E compares with form A as follows:

$$\frac{M''_E}{M''_A} = \frac{0.856}{0.51} = 1.68$$

This tube form gives the greatest increase in charge over the simple tube of form A. This result is not directly comparable with the results for forms B and C, because in form E the tube cross section is reduced by 75 percent but in the other forms only by 50 percent.

(e) Increase of cross section at open end of tube (form F):

The adverse effect of a reduction of cross section at the exhaust end having been shown, the question arises, whether an increase of cross section at the end of the tube is desirable.

In figure 18 it may be seen that the first waves traveling to the right, waves a and c, are reflected at the point of increase of cross section with reversed signs as waves d and e and that by these waves a short intake process and an explosion are effected, the fresh charge column ξ'' being drawn in during the period $\tau_E - \tau_A$ and exploded.

At the open end of the tube, the original waves a and c are reflected with reversed signs as in the normal case, giving rise to the rarefaction wave f and the subsequent condensation wave g. Although these waves encounter the pressure wave arising from the ignition of the column of fresh charge ξ'', they likewise effect an intake process and an explosion, the fresh charge column ξ''' being drawn in during the period τ'_A to τ'_E.

Thus the remarkable circumstance exists that during one working cycle of the tube, intake and explosion occur twice. Comparing the intake quantities M'' and M''' contained in the columns of fresh charge ξ'' and ξ''' with the normal case of the cylindrical tube in figure 11, it is found that during the first period, τ_A to τ_E, 45 percent less is drawn in but in the second period, τ'_A to τ'_E, 40 percent more is drawn in; the charge is therefore almost doubled by this increase in the cross section. Of course the doubled frequency of opening of the valves must be regarded as unfavorable to their length of life.

INVESTIGATION OF A STREAMLINED TUBE

(Argus VSR 9z, Drawings II 11039 and II 11036)

This tube has a form selected as aerodynamically advantageous. Its realization was very earnestly desired as a means of reducing the air resistance, which with the cylindrical jet tube is excessive. It will be shown that from a gas-dynamic aspect, the ability of this cigar-shaped tube to operate is very doubtful. Tests have meanwhile confirmed this: The tube proved itself incapable of operation on the test stand. The investigation of this tube affords a practical application of the arguments set forth.

In accordance with the method of substituting discontinuous for continuous changes, the longitudinal cross section of the tube is approximated by a step-curve with three steps. At each step the ratio of the smaller to the larger cross section is 0.63.

Because it is a question of an approximation, there remains a certain leeway as to how the real form shall be approximated by the step-curve. For practical reasons, two step-curves representing two extremes were chosen; one (figs. 19 and 20) in which the step-curve lies on the outside of the real shape; and another (fig. 21) in which it lies inside the real shape.

With these two step-curves two limiting cases between which the real shape lies may be investigated. The investigation of the limiting cases has this advantage, that from their different gas-dynamic behavior, it can be deduced how the given streamline form may be improved by slight alterations. This process is particularly facilitated by figure 22, where for each step-curve a mean continuous curve is given, between which the actual shape lies. The investigation will show which of these limiting continuous curves must be approached in order to improve the gas dynamics of the streamlined tube as far as possible, or, for that matter, to make the streamlined tube operable at all, because it should be pointed out at once that the operability of the streamlined form as given is open to doubt because of the marked constriction at the end of the tube.

In order to make possible a comparison between this investigation and the results obtained earlier for the cylindrical tube of figure 11, the ratio of the effective inlet cross-sectional area to the tube cross-sectional area at the valve plate shall be disregarded and as the parameter the ratio of the effective inlet cross-sectional area to the maximum cross-sectional area of the tube, namely, $F_E/F_R = 0.4$, shall be taken. As the initial condition at the beginning of the working

cycle, it is again assumed that the tube is charged for 1/7 of its length with fresh charge, which is under an initial pressure of 2.5 times atmospheric pressure, corresponding to a ratio of sonic velocities of 1.144.

In order to keep the investigation from becoming unduly complicated, in figures 19 and 21 each rarefaction wave will again be represented by a single rarefaction line. In figure 20 the rarefaction waves for the case corresponding to figure 19 are shown in better approximation by means of two lines, as a check on whether the approximation by one line is sufficiently exact.

Let the step-curve shown in figure 19 now be investigated. Here the last abrupt change in cross section takes place at the end of the tube. The condensation shock wave in passing through the changes of cross section gives rise to condensation waves traveling in the opposite direction; at the same time it is so strengthened that the gas leaves the tube with a pressure greater than atmospheric and at the velocity of sound (condition 8).

The conditions at the end of the tube are now such that for all practical purposes the condensation shock wave is not reflected at all. This is of serious consequence for the operation of the tube because the automatic operation of the tube depends directly on the reflection of the condensation shock wave from the end of the tube as a rarefaction wave and on the opening of the inlet valves by this returning rarefaction wave. As this reflected rarefaction wave is now lacking, the valves are not opened at all and the tube thus cannot function.

Similar considerations apply to the subsequent rarefaction wave c. It is reflected as a rarefaction wave at the changes of cross section within the tube, simultaneously strengthened by entry into the narrower sections of the tube, and not reflected at the open end of the tube so the reflected condensation wave, which in its return would ignite the new charge, likewise does not arise.

The waves reflected at the changes in cross section within the tube are also not capable of maintaining the automatic operation of the tube, for the waves reflected are always of opposite sign to those required for operation, that is, a rarefaction wave instead of a condensation wave and vice versa. Furthermore, the reflected waves eventually so overtake each other and cancel that after only one cycle of reverberation the atmospheric condition of rest is restored.

By means of figure 20, it is now inquired whether this negative result is due to the rough approximation of the rarefaction wave by a single rarefaction line b. In figure 20 therefore, the rarefaction wave is represented more exactly by means of two rarefaction lines, as originally done for the cylindrical tube. This subdivision certainly has no influence on the condensation shock wave a and it is therefore exactly as in figure 19, reflected at the exhaust end of the tube not as the required rarefaction wave but as a very weak condensation wave, which in practice may be disregarded.

Now it could be possible that by reflection at the intermediate changes of cross section, waves might arise that would support the automatic operation of the tube. It is found, however, that even with this more accurate representation the reflected waves d to i create no subatmospheric pressure at the intake and consequently the valves are not opened. The lowest pressure that occurs at the inlet end is that of the atmosphere, exactly as in figure 19; the two figures likewise agree in respect to maximum pressure. The simplified conception of the form of the rarefaction wave is therefore not the cause of the negative result.

The investigation of the second step-curve is illustrated in figure 21. At the exhaust end there is not a point of choking but a cylindrical portion of the tube; the individual drops in cross section are shifted toward the left as compared to the first step-curve. The investigation gives significantly better results in this case. The condensation shock is again strengthened in passing through the drops in cross section and now, because the exhaust portion of the tube is cylindrical, it is reflected as a rarefaction wave. The strengthening of the condensation shock wave in passing through the drops in cross section produces a strong reflected rarefaction wave and an outward flow of the gas from the tube at the velocity of sound. This reflected rarefaction wave, due to its strength, produces upon arrival at the inlet end a strong intake action having a gas velocity of 0.2 and a subatmospheric pressure corresponding to a velocity of sound equal to 0.976 (condition 39, table VIII). A comparison with the cylindrical tube shows that the corresponding values for the cylindrical tube are: gas velocity, 0.34; velocity of sound, 0.924. The intake conditions for the second step-curve are therefore less favorable than for the cylindrical tube.

The subsequent rarefaction wave c, being likewise strengthened at the drops in cross section, is reflected as a relatively strong condensation wave l from the exhaust end of the tube; but the strength of this wave is disadvantageous here, as its strength involves a high

velocity of propagation and consequently it does not arrive at the intake area late enough after the rarefaction wave to allow enough fresh charge to be drawn in. Because of this, in comparison with the cylindrical tube only 74 percent as great a quantity of fresh charge is drawn in.

The waves reflected from the points of change of cross section, as these points are encountered by the original waves a and c, exhibit no effect upon the mode of operation of the tube, because they cancel each other rather quickly certainly before the rarefaction wave arising from the reflection of the condensation shock wave at the tube mouth passes back through the constrictions.

The step-curves may be regarded as approximations of mean curves that depart somewhat from the given longitudinal section: the one curve (outer step-curve) in the sense that it is more rounded-in at the exhaust end; the other curve (inner step-curve) in the sense that it is more elongated and cylindrical at the exhaust end. These mean curves are compared with the actual tube form in figure 22. On the basis of the results obtained, the more rounded-in form must be considered out of the question. With this form the automatic operation of the tube must be considered impossible. The more nearly cylindrical form ought to be operable, especially in flight, where the intake conditions are more favorable than in the stationary test setup that has been considered.

In any case the comparison of the three tube forms shown in figure 22 shows how sensitive is the automatic operation of the tube to the influence of the shape of its exhaust end, because the exhaust ends of the three shapes actually differ relatively little. Unquestionably, the end of the tube must be as cylindrical in form as possible. In other words, it may also be said that although the cigar-shaped streamlined form shows itself in tests to be unsuitable for automatic tube operation, it may be improved by slight changes at the exhaust end of the tube, such as by the addition of a cylindrical portion to the tube; of course, a gradual transition from cigar to cylinder shape must be provided.

MODE OF OPERATION OF JET TUBE IN FLIGHT

General considerations.

In the case of the tube in flight, the simplified consideration in terms of adiabatic processes need be modified by only one new condition, namely, that the outside pressure on the inlet valves is the

impact pressure. It is presupposed that the full effect of the impact pressure is directed against all valves by suitable fairing (total head scoop).

The impact pressure is computed from the Bernoulli equation for a compressible flow

$$\frac{a_1^2}{\kappa - 1} + \frac{u^2}{2} = \frac{a_s^2}{\kappa - 1}$$

in which a_s = velocity of sound at stagnation point and a_1 = velocity of sound in the undisturbed atmosphere. As before, all velocities are made dimensionless by dividing by the velocity of sound a_1. Be it particularly noted that a_1 refers not to ground level but to the altitude of flight at the moment in question.

A further assumption is that even under the full effect of the impact pressure, the valves maintain gas-tight closure and that, upon the arrival of the reflected rarefaction wave at the inlet end of the tube, they at once completely open. This assumption does not exactly correspond to the facts because the valve flaps must be held forward with spring pressure in order to remain closed against the force of the impact pressure. Hence, they will be opened by the wave of lower pressure only so wide as corresponds to the additional load imposed by the lower pressure, which at various flight speeds will naturally vary in proportion to the impact pressure. The investigation of this influence of the strength of the valve springs on the opening of the valves, however, will be postponed until later.

In treating the wave reflection at the valves, it must be noted that the velocity of sound of the stagnation point a_s and not that of the atmosphere a_1 now applies to the ellipse in figure 8 $u = 0$.

Influence of flight speed on amount of charge.

The investigation will be carried out for

$$\frac{F_E}{F_R} = 0.2 \quad \text{and} \quad \frac{F_E}{F_R} = 0.4$$

again with $\xi' = 1/7$ and $a'/a_1 = 1.144$.

The individual wave diagrams, which were drawn for flight speeds of 0.3, 0.45, 0.55, 0.78, and 1.00 times the velocity of sound, are not given in the appendix; simply the results in figures 23 and 24 are given, first as the ratio of the quantity of fresh charge M" newly drawn in to the quantity M' originally present plotted against flight speed and then as the ratio of M" at the given flight speed to the quantity M''_0 corresponding to zero flight speed plotted against flight speed.

As the impact pressure increases, a point is reached at which the gas velocity in the valve cross section F_E is equal to the speed of sound. With a further increase in impact pressure this critical state persists, because with the chosen valve construction no supersonic speed can arise. Nevertheless the quantity of inflowing gas continues to increase because at a pressure ratio above the critical the gas quantity depends solely on the state of the gas on the pressure side of the valves. Thus, rarefaction waves arriving from the open end of the tube and striking the valves after the critical condition has been reached have no further effect on the quantity of gas flowing in.

The presentation of the results in figures 23 and 24 shows that with increasing flight speed the quantity of new charge flowing in increases slowly at first and then more and more markedly. Figure 23 also shows the obvious fact that with $F_E/F_R = 0.4$ the inflow is consistently greater than with $F_E/F_R = 0.2$. In the terms of figure 24, the percentage increase is the same whether $F_E/F_R = 0.2$ or 0.4.

Influence of leakiness of valves.

Figure 10 shows that when $F_E/F_R = 0.2$, the minimum pressure occurring at the inner side of the valves corresponds to the ratio $a/a_1 = 0.896$. The pressure corresponding to this is $\left(\frac{a}{a_1}\right)^{2\kappa/(\kappa-1)} = 0.464$; that is, the ratio of the absolute pressure to the atmospheric pressure. The pressure difference at the valves amounts thus to 54 percent of the atmospheric pressure.

On the other hand, for a tube flying at 0.64 of the velocity of sound, the ratio of impact pressure to atmospheric pressure = 1.32. Now it has been seen from the preceding investigations that atmospheric pressure is attained behind the pressure wave as it travels out of the tube. Between the explosion and the subsequent intake there is atmospheric pressure on the inner side of the valves, so that a pressure

difference at the valves of 32 percent of atmospheric pressure then exists. During the intake period, a maximum pressure difference of 54 + 32 = 86 percent of atmospheric pressure exists.

The fixed tube and the tube in flight shall now be compared under equal atmospheric conditions. If at rest, the valves open to the degree $F_E/F_R = 0.2$ at the maximum, that is 54 percent pressure difference; then in flight they open at the same low pressure approximately to the degree $F_E/F_R = 0.2 \frac{86}{54} = 0.32$. During the interval in which atmospheric pressure exists on the inner side of the valves at rest, the valves are closed but in flight they are open approximately to the degree $F_E/F_R = 0.2 \frac{0.32}{0.54} = 0.12$. This opening is designated the leakiness. Relative to the maximum opening it amounts to $\frac{0.12}{0.32} = 37$ percent.

It is thus seen that at sufficiently high flight speeds, the valves are constantly open excepting of course at the time of explosion. It shall now be investigated how the jet tube reacts to this condition.

Inasmuch as no exact data on valve opening exist, the effects of a leakiness of 50 percent and of 100 percent shall be investigated with the assumptions of maximum attained valve opening $F_E/F_R = 0.2$ and flight speed of 0.64 of the velocity of sound.

The investigation is made by means of figures 25 and 26. The only difference from the earlier case shown in figure 10 is that from the instant τ', when the outward traveling rarefaction wave leaves the valves, fresh charge begins to flow in through a cross-sectional area $\Delta F_E/F_R = 0.1$ (fig. 25) or 0.2 (fig. 26). The boundary of the inflowing fresh charge is again shown by a finely dotted line. For the succeeding intake period it is assumed that the mechanical limit to the valve-opening area is $F_E/F_R = 0.2$ and that it is attained. In reality, of course, the opening area depends upon the pressure head, which varies during the intake period; it would scarcely be worth the effort, however, to take account of the consequent alteration from moment to moment of the effective inlet area.

If the cases of figures 25 and 26 are compared as to the quantities of fresh charge available for the second working cycle, that is, the quantities present at the moment τ_E, figure 27 is obtained, which shows the increase with increasing leakiness. From this figure it can be seen that the increase of the quantity of fresh charge due

to a slight leakiness of the valves is quite advantageous but that greater leakiness results in a too great increase in the charge, in the sense that a sufficiently rapid spread of ignition throughout the gas becomes doubtful and also that too great a cooling of the tube may be expected.

In order to evaluate the operability of the tube with valve leakiness, the strength of the returning wave must be considered. The investigation shows that the leakiness does not affect the low pressure created at the valves by the returning rarefaction wave, the suction effect thus remaining the same but that the returning condensation shock wave is somewhat weakened. The decrease of the pressure ratio (ratio of pressure after to pressure before the shock) produced by the compression shock wave is shown in figure 28. The reason for this effect is, that whereas the outward-traveling condensation shock wave a is unaffected, consequently the rarefaction waves d and e arising from it by reflection are unaffected; on the other hand, the outward traveling rarefaction waves b and c, and also the condensation shock wave f arising from them by reflection, are weaker because the gas condition 7 behind the outward traveling wave possesses a higher pressure than it would at zero leakiness. The decrease of the pressure ratio in the shock wave f is 20 percent at 100 percent leakiness, according to figure 28.

Furthermore, it is found that the rarefaction waves g and h reflected from the valves become stronger with increasing leakiness without, however, giving rise to any negative gas velocities (that is, inflow at the exhaust end near the end of the working cycle).

A limited leakiness has an advantageous effect inasmuch as it increases the weight of new charge induced and only slightly affects the waves. Greater leakiness results in a weakening of the returning compression shock and therefore has an unfavorable effect on the ignition, as does also the cooling of the tube and the less rapid spread of ignition throughout a larger as compared to a smaller quantity of fresh charge.

INFLUENCE OF COMBUSTION PRESSURE

Although the influence of the combustion pressure is of less practical significance because its magnitude cannot be predetermined, for instance by the choice of fuels, it is nevertheless of interest inasmuch as according to the research of Busemann (reference 5) the best yield of work from a thermodynamic viewpoint is secured from a jet tube with combustion at constant volume and the question arises, whether the jet tube is operable with this kind of combustion.

Combustion at constant volume is characterized by a higher combustion pressure than normally occurs in the pulse-jet tube. It will therefore be possible to decide the question approximately by investigating the influence of the combustion pressure.

The results of the investigation are shown in figure 29. According to this figure, the degree of charge and the pressure ratio in the reflected compression shock at first increases with increasing combustion pressure p then reaches a maximum in the neighborhood of which the curves are level and thereafter decrease, so at too high a combustion pressure, in this case namely at $p/p_1 > 7$, the operability of the tube becomes questionable.

The reason is that with increasing combustion pressure a point is reached at which the exhaust flow reaches the velocity of sound and beyond that point the outward-traveling explosion wave is no longer reflected at full strength as a rarefaction wave because the reflected wave has zero net velocity of propagation against the gas flowing out with the velocity of sound. This reflected wave remains at the mouth of the tube and is only disposed of by the subsequent arrival of the rarefaction waves b and c, as a result of which these waves are in part reflected as rarefaction waves and not condensation waves as they should be; consequently the reflected compression shock is weaker.

From equation (1), the combustion pressure at which the exhaust will reach the speed of sound can easily be computed. The sound velocity attained at the exhaust end is then that of the surrounding atmosphere. Letting a_v be the sound velocity corresponding to the combustion pressure, then on the one hand

$$\Delta a = a_v - a_1$$

on the other hand

$$u = \frac{2}{\kappa - 1} \Delta a = a_1$$

and therefore

$$a_v = \frac{\kappa - 1}{2} a_1 + a_1 = 1.2\, a_1$$

$$\frac{a_v}{a_1} = 1.2$$

or

$$\frac{p}{p_1} = 3.6$$

But the pressure occurring in the jet tube is actually $p/p_1 = 2.5$.

INFLUENCE OF TUBE FORM ON VARIATION OF PRESSURE WITH TIME AT VARIOUS TUBE CROSS SECTIONS

In order to make a comparison with measurements of the sequence of pressures taken through taps in the tube walls, the theoretical sequences of pressures at the points $\xi = 0.4$ and $\xi = 0.6$, that is at distances of 0.4 and 0.6 of the tube length from the inlet end, were derived from the wave diagrams of figures 11, 14, and 15, corresponding to the tube forms A, B, and C of figure 13. The results are shown in figures 30, 31, and 32 for one working cycle. These figures show the ratio of tube pressure to atmospheric pressure p_1 plotted against dimensionless time τ. The arrows above the waves indicate their direction of propagation in the tube.

In comparing the cylindrical tube, form A (fig. 30), with that having the enlarged combustion chamber, form B (fig. 31), it is noteworthy that the pressure varies less widely for form B than for form A. This fact had been observed in the experimental measurements and had then led to the opinion that a less vigorous combustion took place in form B. But it is now apparent that the cause lies entirely in the tube form. As to form C, figure 32 shows that a constriction half-way along the tube gives rise to additional pressure peaks. In this case, the outward-traveling and inward-traveling waves are not separated by a time interval as in the preceding tube forms, a circumstance that makes the evaluation of experimental measurements more difficult.

REFERENCES

1. Ackeret, J.: Gasdynamik. Bd. VII, Kap. 5 of Handbuch d. Phys., H. Geiger and K. Scheel, ed., Julius Springer (Berlin), 1927, pp. 289-342. (British R.T.P. Trans. No. 2119, Ministry Aircraft Prod.)

2. Sauer, R.: Ing.- Archiv, Bd. XIII, 1942, p. 79.

3. Schultz-Grunow, F.: Forsch. Ing.- Wes., Bd. 13, Heft 3, 1942, p. 125.

4. Schultz-Grunow, F.: Ing.- Archiv, Bd. XIV, Heft 1, 1943, pp. 21-29, ("Non-Steady, Spherically-Symmetrical Gas Motion and Non-Steady Gas Flow in Nozzles and Diffusors." British R.T.P. Trans. No. 2071, Ministry Aircraft Prod.)

5. Busemann, A.: FB 530, ZWB.

TABLE I

STATE VALUES FOR FIGURES 10 AND 11

$F_E/F_R = 0.2$			$F_E/F_R = 0.4$		
Number	a/a_1	u/a_1	Number	a/a_1	u/a_1
1	1.000	0	1	1.000	0
2	1.072	.36	2	1.072	.36
3	1.036	.18	3	1.036	.18
4	1.144	0	4	1.144	0
5	1.108	.18	5	1.108	.18
6	1.072	0	6	1.072	0
7	1.036	.54	7	1.036	.54
8	1.000	.72	8	1.000	.72
9	1.000	.36	9	1.000	.36
10	.964	.54	10	.964	.54
11	1.000	.36	11	1.000	.36
12	.964	.18	12	.964	.18
13	.928	.36	13	.928	.36
14	.964	.18	14	.964	.18
15	.954	.13	15	.970	.21
16	.918	.31	16	.934	.39
17	.896	.20	17	.922	.34
18	.990	-.05	18	1.006	.03
19	.968	-.16	19	.998	.02
20	.954	.67	20	.970	.52
21	.910	.910	21	.922	.85

TABLE II - STATE VALUES FOR FIGURE 14

Form B

Number	a/a_1	u/a_1	Number	a/a_1	u/a_1
1	1	0	14	0.911	0.445
2	1.144	0	15	.960	.200
3	1.089	.445	16	.928	.530
4	1.105	.205	17	.954	.230
5	1.062	0	18	.959	.255
6	1.042	.100	19	1.007	.017
7	1.04	.200	20	1.007	.035
8	.951	.645	21	1.017	.085
9	1	.890			
10	1	.400			
11	1.022	0			
12	1.015	.035			
13	1.015	.070			

TABLE III - STATE VALUES FOR FIGURES 15 AND 16

Form C						Form D		
Number	a/a_1	u/a_1	Number	a/a_1	u/a_1	Number	a/a_1	u/a_1
1	1	0	14	0.961	0.685	1	1	0
2	1.144	0	15	.970	.150	2	1.144	0
3	1.072	.360	16	.954	.230	3	1.072	.36
4	1.102	.210	17	1.018	.090	4	1.080	.32
5	1.088	.440	18	1.049	.245	5	1	.965
6	1	.880	19	1	.180	6	1.008	-.04
7	1.030	-.150	20	1.031	.335			
8	1.060	0	21	1	.490			
9	.912	.440	22	.969	.335			
10	1	.300	23	.982	.090			
11	.954	.230	24	.951	.245			
12	.930	.530	25	1.012	.060			
13	.984	.380	26	1	.018			

TABLE IV - STATE VALUES FOR FIGURE 17

Form E

Number	a/a_1	u/a_1	Number	a/a_1	u/a_1
1	1	0	27	1.029	-0.017
2	1.144	0	28	1.026	-.035
3	1.103	.205	29	1.017	-.075
4	1.069	.445	30	1.007	-.025
5	1.129	.245	31	.995	.473
6	1.108	.540	32	.950	.260
7a	1.013	.013	33	.980	.110
7b	1	1	34	1	0
8	1.082	0	35	1	.200
9	1.042	.100	36	1.020	.100
10	1.040	.200	37	1	.210
11	1.080	0	38	.969	.360
12	1.055	.125	39	.924	.570
13	1.050	.250	40	.950	.250
14	.955	.723	41	.926	.310
15a	1.013	.433	42	.970	.150
15b	1	.51	43	.978	.190
16	1.022	0	44	.986	.190
17	1.049	.082	45	1.016	.040
18	1.015	.075	46	1.013	.010
19	1.055	-.125	47	1.013	.010
20	1.030	0	48	1.015	.035
21	1.020	.050	49	1.013	.080
22	1.020	.100	50	.998	.180
23	.925	.573	51	1.042	-.2
24	.970	.360			
25	1	.210			
26	1.042	-.100			

TABLE V - STATE VALUES FOR FIGURE 18

Form F

Number	a/a_1	u/a_1	Number	a/a_1	u/a_1
1	1.000	0	12	0.484	-0.08
2	1.144	0	13	.956	.20
3	1.072	.36	14	.998	-.01
4	1.03	.57	15	.914	.41
5	1.054	.27	16	1.070	.35
6	1.000	.54	17	.986	.77
7	1.000	.54	18	1.070	.35
8	.946	.27	19	.916	.42
9	.966	.21	20	.908	.39
10	.916	.42	21	.992	-.03
11	.930	.18			

TABLE VI - STATE VALUES FOR FIGURE 19

Number	a/a_1	u/a_1
1	1	0
2	1.144	0
3	1.072	.36
4	1.094	.25
5	1.084	.420
6	1.11	.29
7	1.096	.48
8	1.022	1.022
9	1.026	-.13
10	1.022	-.11
11	1.044	0
12	1.022	.11
13	1.02	-.1
14	1.02	-.16

TABLE VII — STATE VALUES FOR FIGURE 20

Number	a/a_1	u/a_1	Number	a/a_1	u/a_1
1	1.000	0	29	0.998	0.02
2	1.144	0	30	1.026	-.13
3	1.072	.36	31	1.010	-.05
4	1.108	.18	32	.980	-.07
5	1.000	0	33	.982	.09
6	1.036	.18	34	1.008	-.04
7	1.094	.25	35	1.008	-.06
8	1.084	.42	36	.998	-.01
9	1.110	.29	37	.984	.06
10	1.096	.48	38	.986	.07
11	1.102	.45	39	.988	.08
12	1.058	.07	40	.988	.06
13	1.044	.14	41	1.030	.07
14	1.044	.22	42	1.022	.11
15	1.070	.09	43	1.042	.01
16	1.054	.17	44	1.030	.07
17	1.054	.27	45	1.022	.11
18	1.038	.36	46	1.008	.04
19	1.022	1.022	47	1.028	-.06
20	1.000	.69	48	1.016	0
21	1.022	-.11	49	1.008	.04
22	1.008	-.04	50	1.020	-.10
23	1.020	-.14	51	1.008	-.04
24	1.020	-.16	52	1.028	.06
25	1.004	-.08	53	1.020	.10
26	.994	-.03	54	1.008	.04
27	.980	.04	55	.988	.08
28	.980	.11			

TABLE VIII - STATE VALUES FOR FIGURE 21

Number	a/a_1	u/a_1	Number	a/a_1	u/a_1
1	1.144	0	22	1.020	-0.10
2	1.072	.36	23	1.004	.02
3	1.094	.25	24	.954	.23
4	1.084	.42	25	.944	.40
5	1.110	.29	26	1.012	.06
6	1.096	.48	27	1.002	.11
7	1.128	.32	28	.990	.05
8	1.110	.55	29	.990	.09
9	1.000	1.10	30	.986	.07
10	.890	.55	31	1.000	.14
11	1.032	-.16	32	1.014	.07
12	1.026	-.13	33	.904	.62
13	1.022	-.11	34	.932	.34
14	1.022	.11	35	.962	.27
15	1.026	.09	36	1.000	.08
16	1.026	.13	37	.968	.16
17	1.260	.13	38	1.008	.04
18	1.026	-.13	39	.976	.20
19	1.004	-.02	40	.992	.04
20	1.020	-.16	41	.962	.06
21	.994	-.03	42	1.144	0

TABLE IX - STATE VALUES

For Figure 25			For Figure 26		
Number	a/a_1	u/a_1	Number	a/a_1	u/a_1
1	1	0	1	1	0
2	1.144	0	2	1.144	0
3	1.108	.18	3	1.108	.18
4	1.072	0	4	1.072	0
5	1.072	.36	5	1.072	.36
6	1.036	.18	6	1.036	.18
7	1.01	.05	7	1.024	.12
8	1.036	.54	8	1.036	.54
9	1	.72	9	1	.72
10	1	.36	10	1	.36
11	.964	.54	11	.964	.54
12	1	.36	12	1	.36
13	.974	.23	13	.988	.30
14	.938	.41	14	.952	.48
15	.974	.23	15	.988	.30
16	.964	.18	16	.964	.18
17	.928	.36	17	.928	.36
18	.904	.24	18	.904	.24
19	.966	-.07	19	.952	0
20	.990	.05	20	.976	.12
21	1	.1	21	1	.24

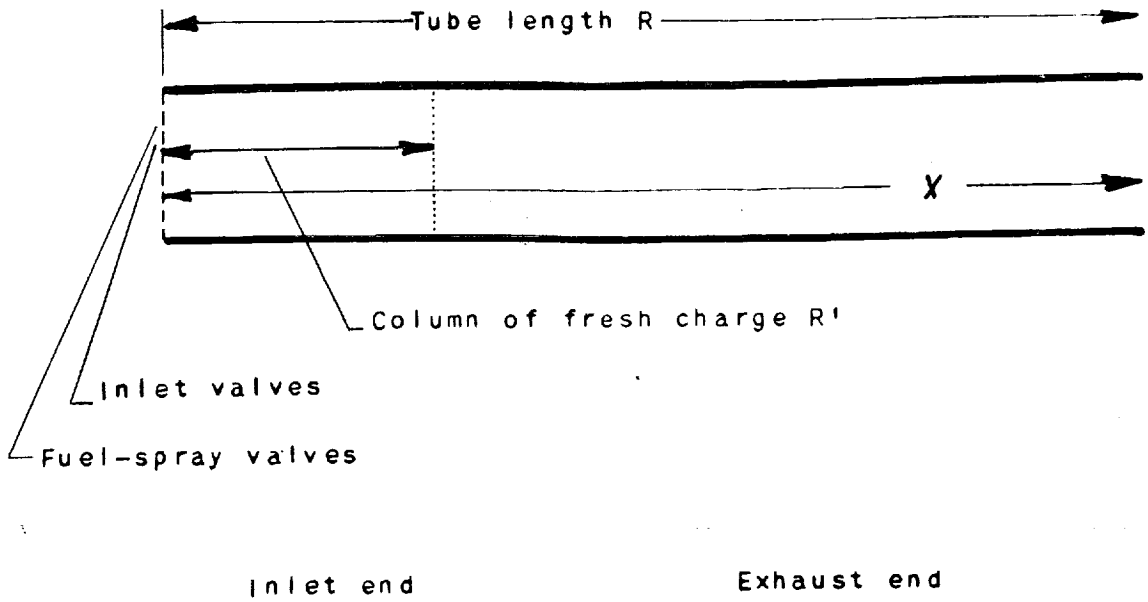

Figure 1. - Schematic diagram of a jet tube.

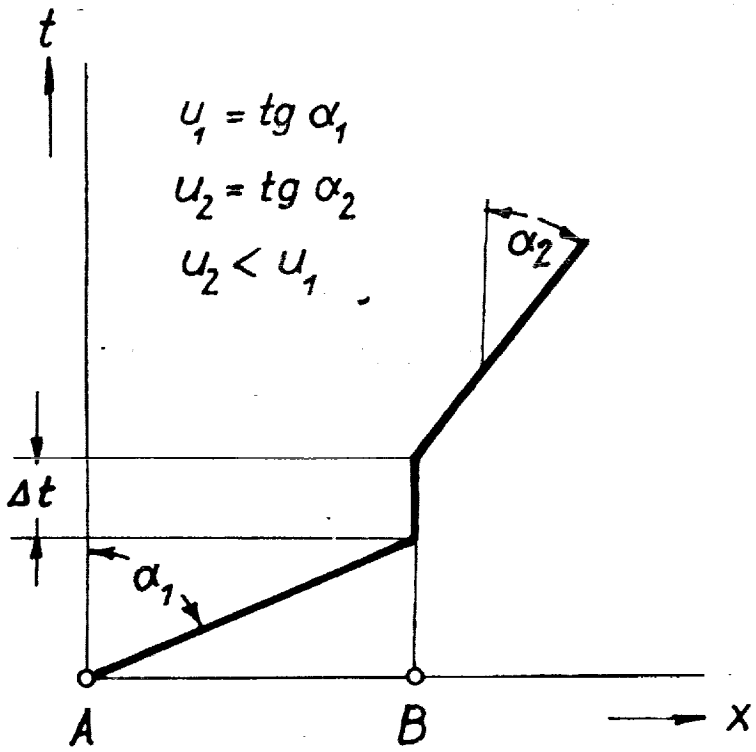

Figure 2. – Graphic representation of a timetable in the t,x diagram.

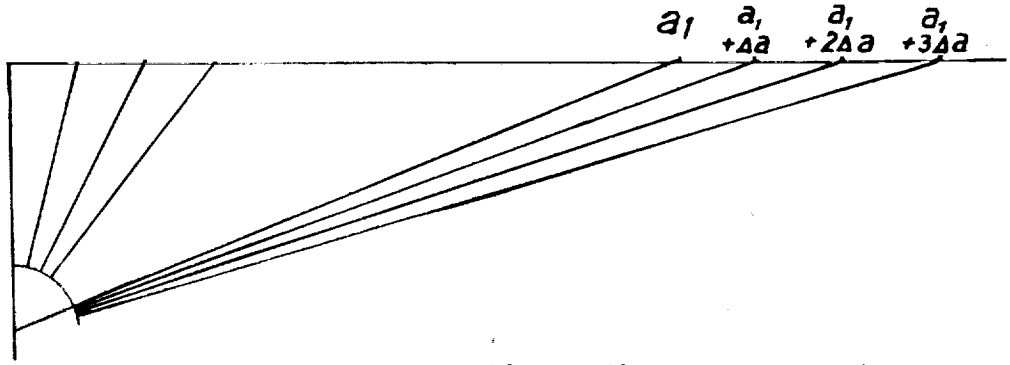

Slope diagram

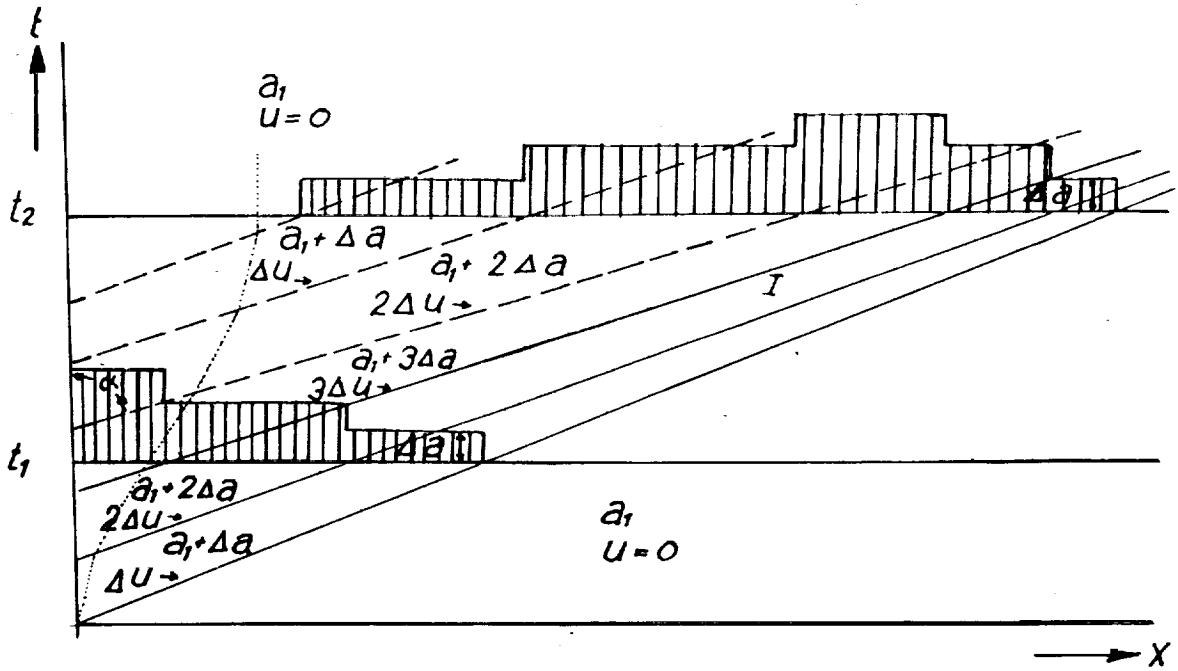

Wave diagram

Figure 3. - Wave propagation in t,x plane. The form at two moments t_1 and t_2 of wave approximately represented by individual wave elements.

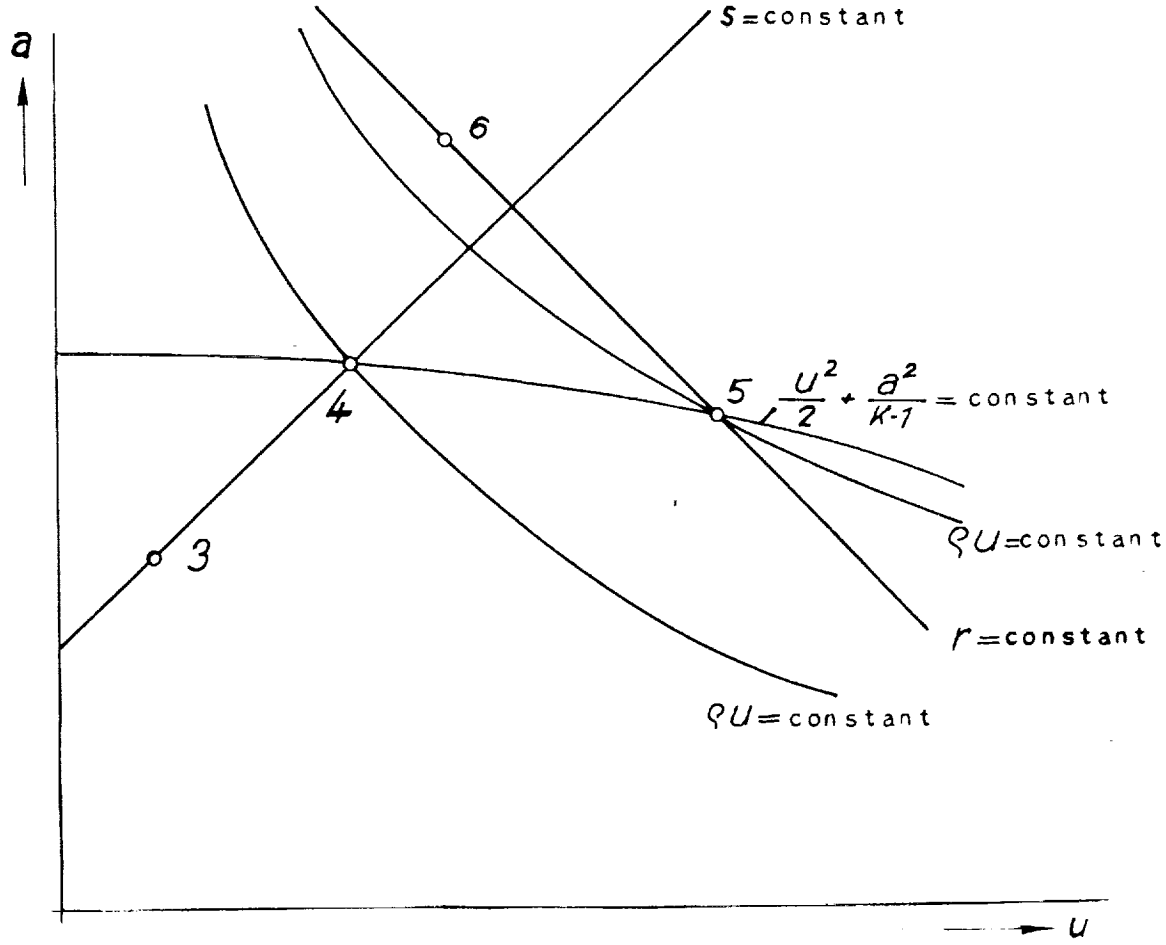

Figure 4. - Passage of a wave through change in cross section as represented in a,u diagram.

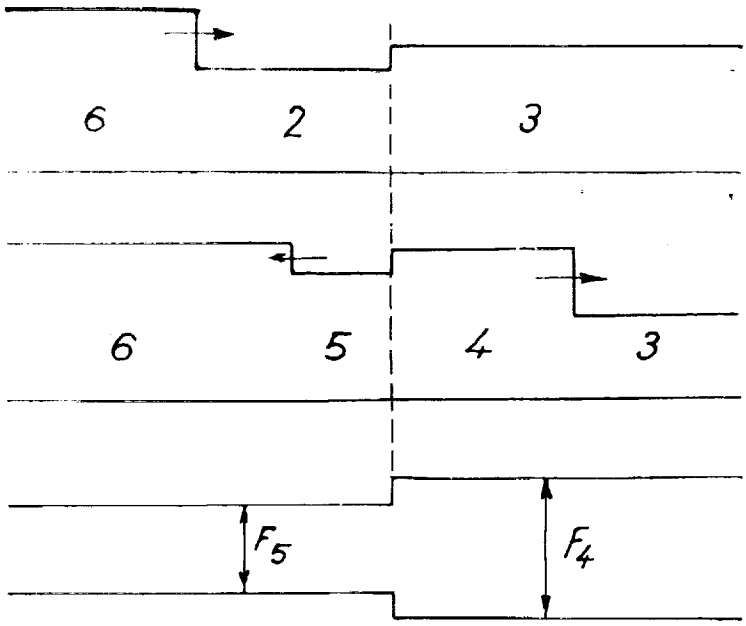

Figure 5. - Passage of a wave through change in cross section. Momentary states.

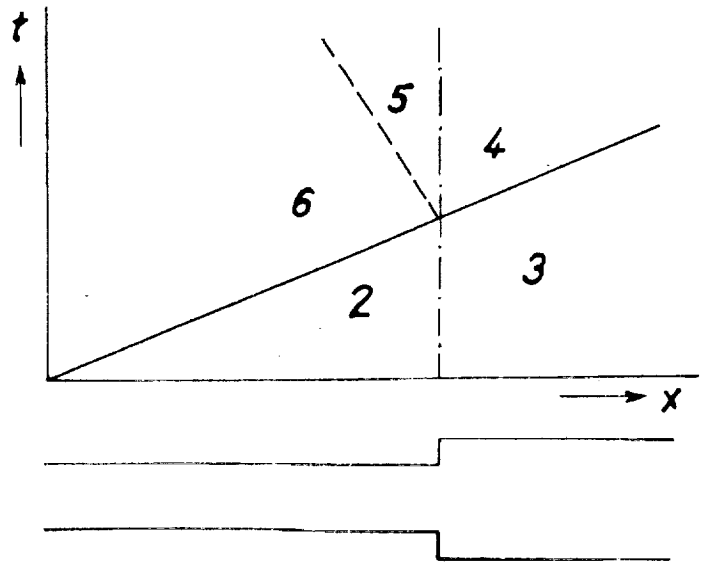

Figure 6. - Passage of a wave through change in cross section as represented in t, x diagram.

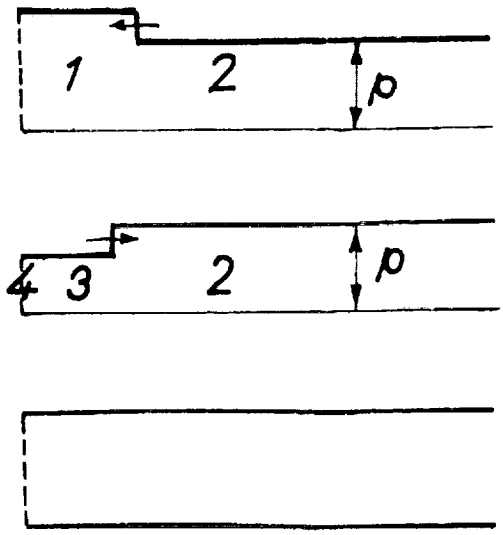

Figure 7. - Reflection of rarefraction wave at inlet valves. Momentary states before and after reflection.

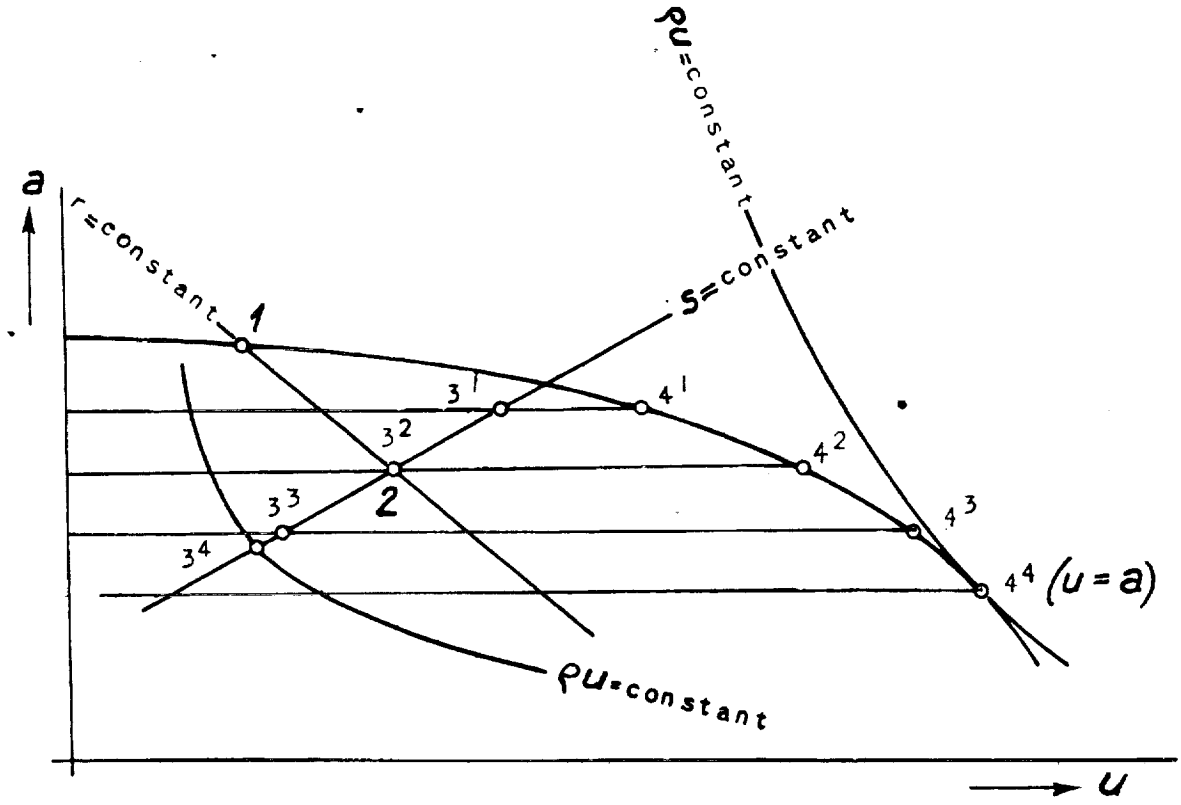

Figure 8. – Reflection of a rarefaction wave at inlet valves. Determination of reflected wave in a,u diagram.

Four cases:

Large valve cross section, reflection of condensation wave 3^1

Smaller valve cross section, no reflection because $3^2 = 2$

Still smaller valve cross section, reflection of rarefaction wave 3^3

Still smaller valve cross section, reflection of rarefaction wave 3^4 and flow through valves at velocity of sound

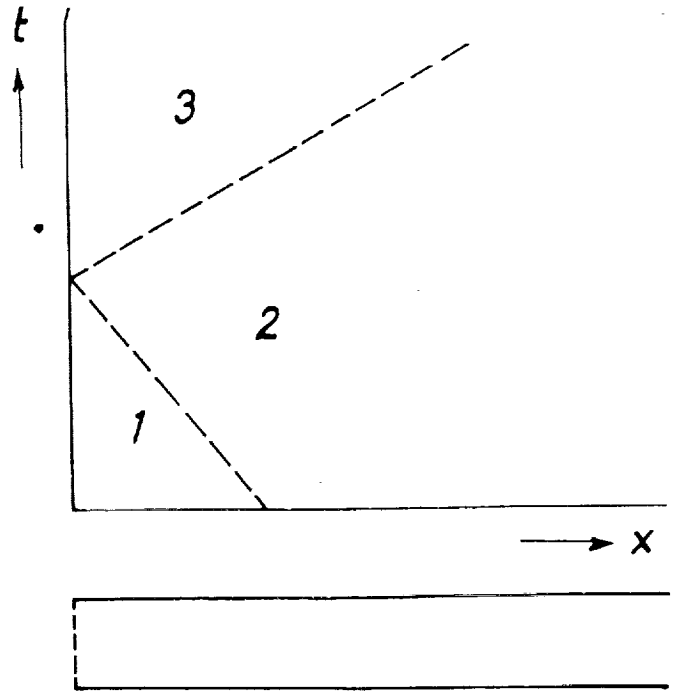

Figure 9. - Reflection expressed in t,x diagram. (To accompany figs. 7 and 8.)

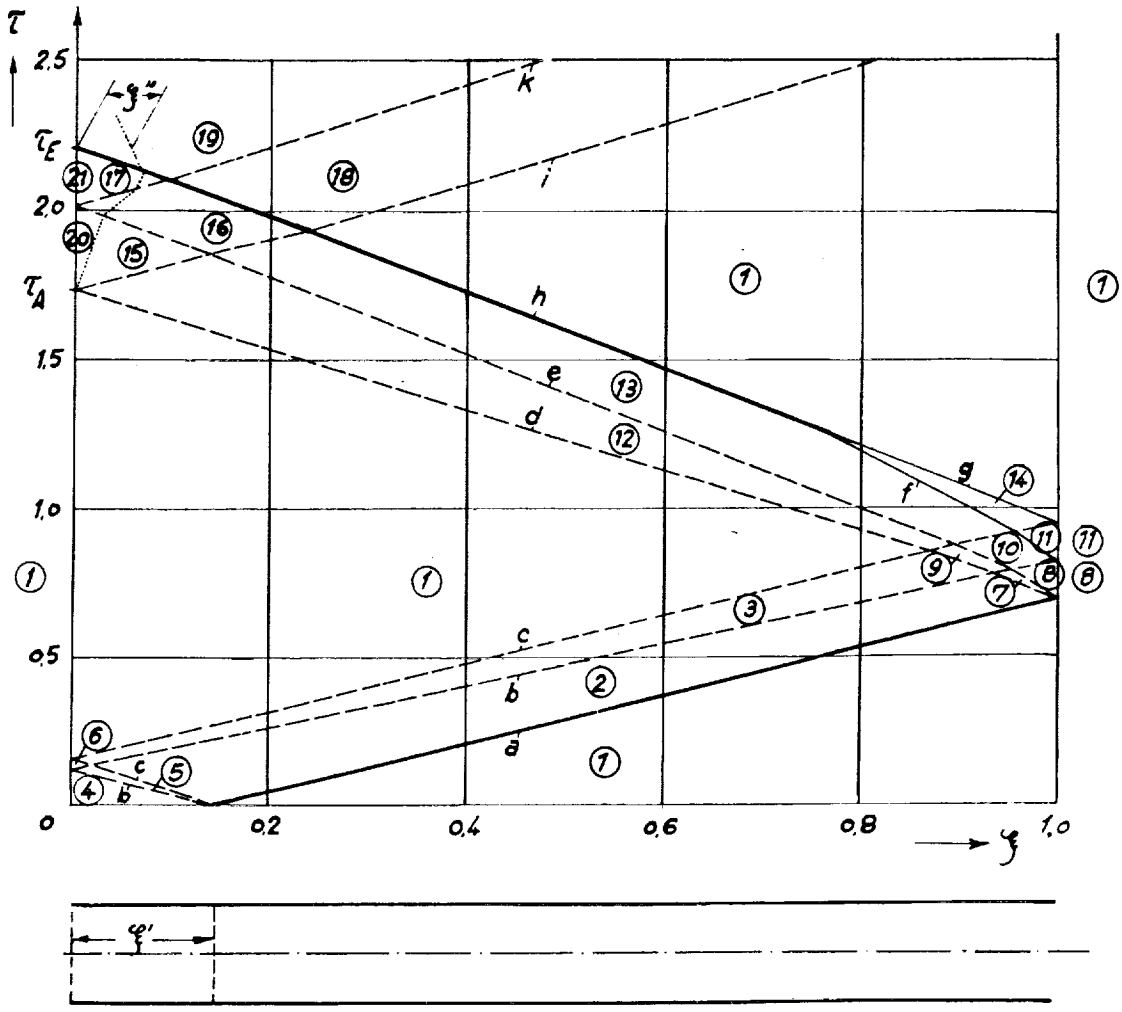

Figure 10. - Wave propagation in jet tube. $F_E/F_R = 0.2$.

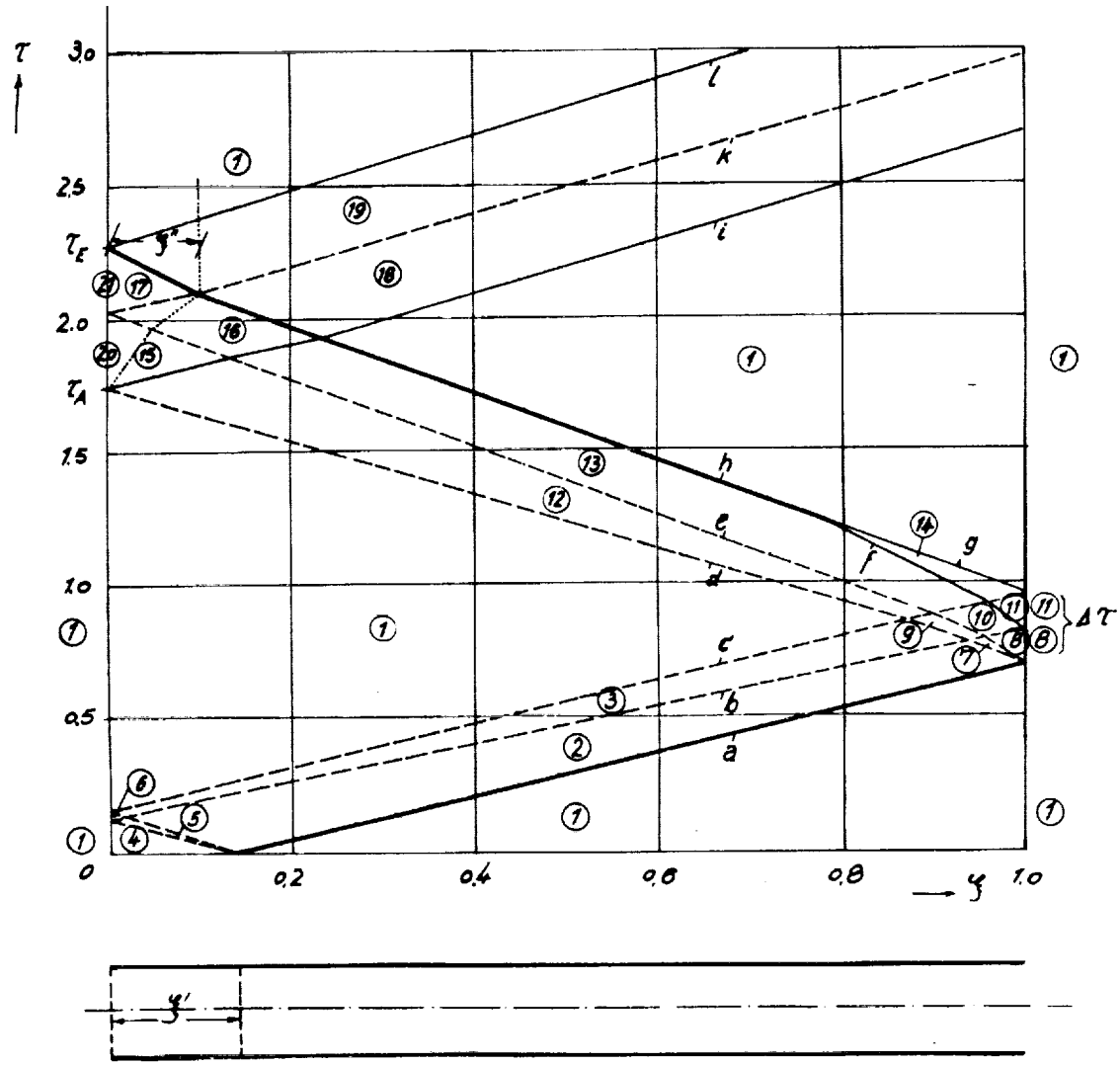

Figure 11. - Wave propagation in jet tube. $F_E/F_R = 0.4$.

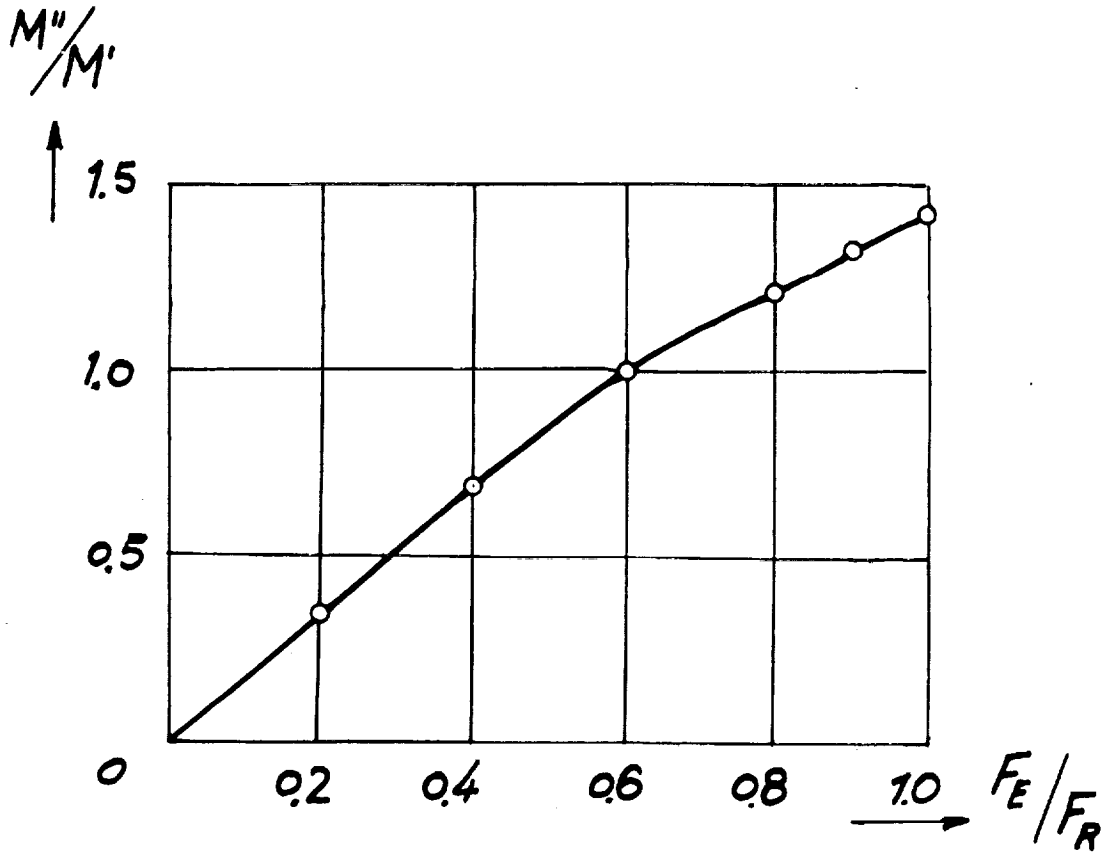

Figure 12. - Ratio of quantity of newly induced charge to quantity originally present as function of F_E/F_R in stationary jet tube.

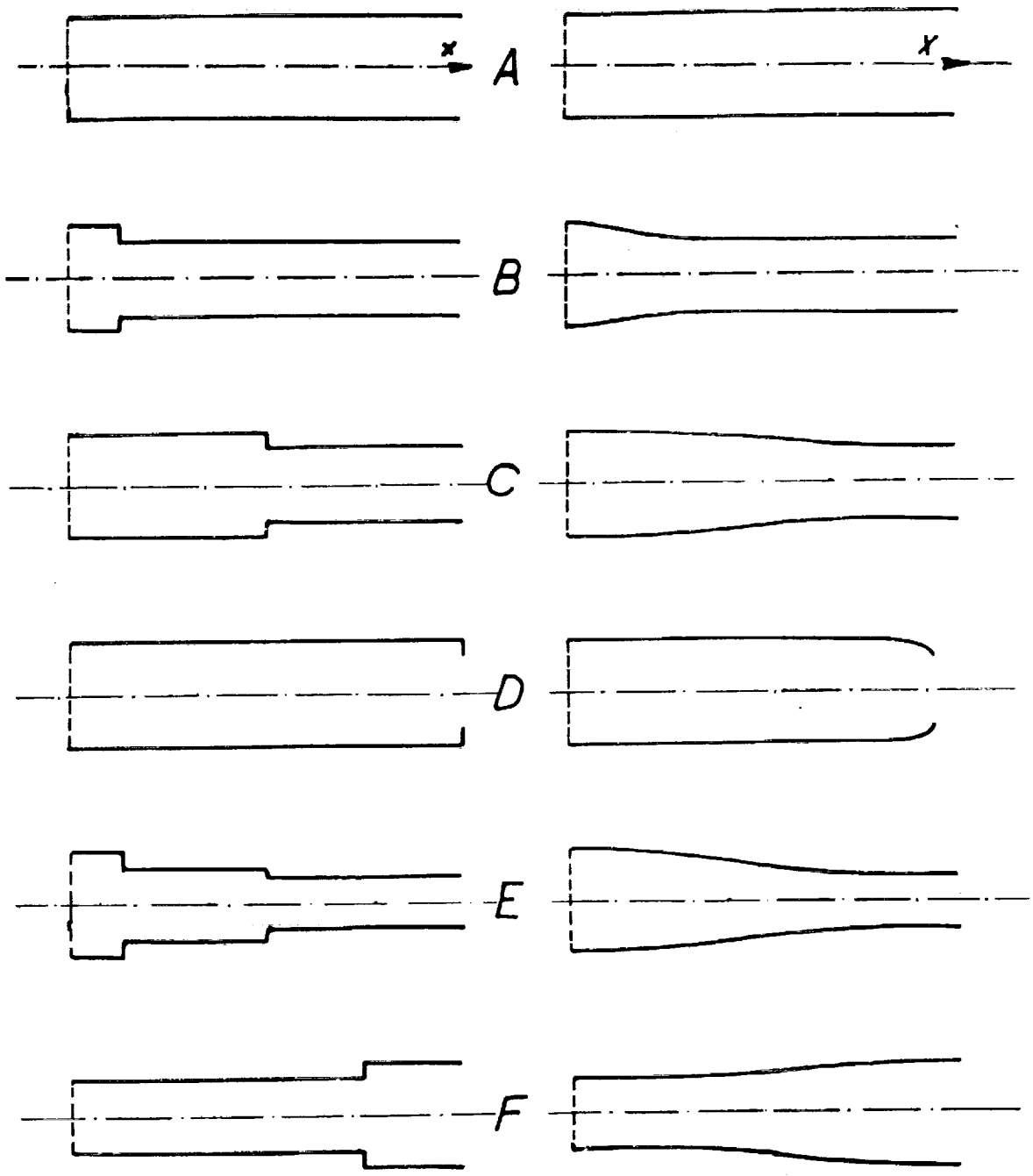

Figure 13. - Tube forms investigated. From left to right each smaller cross section is 50 percent of the preceding one.

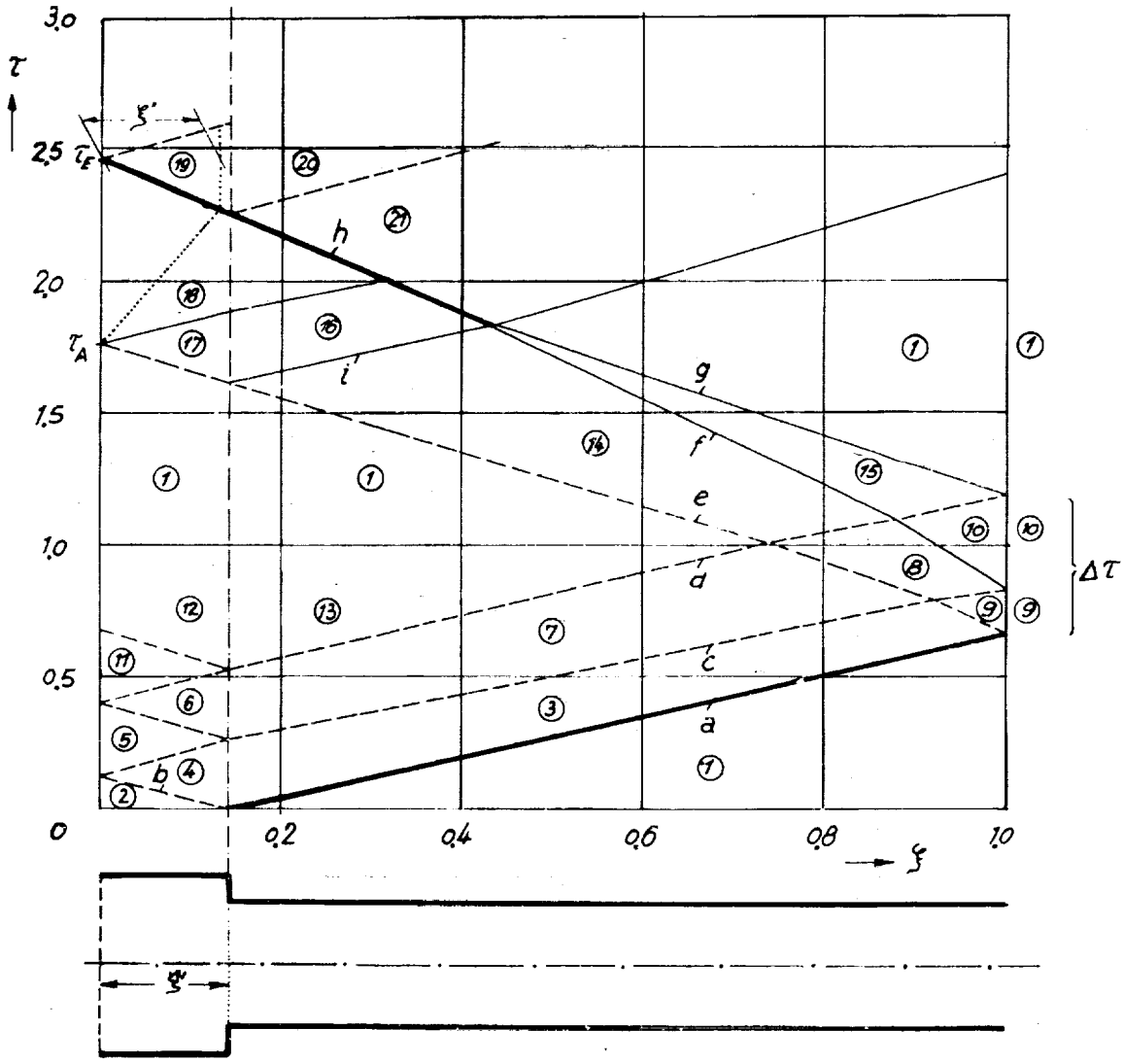

Figure 14. - Wave propagation in the jet tube. $F_E/F_R = 0.4$; form B.

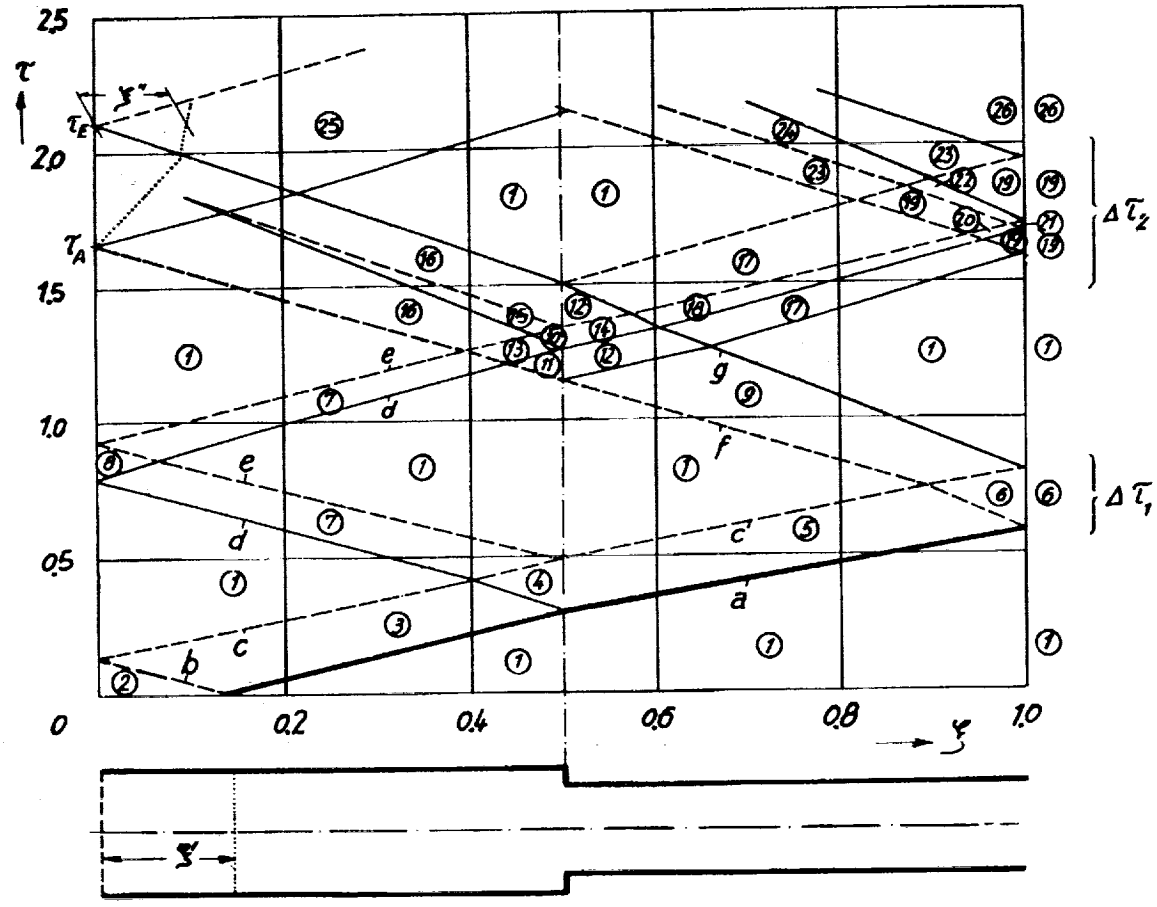

Figure 15. - Wave propagation in jet tube. $F_E/F_R = 0.4$; form C.

621.

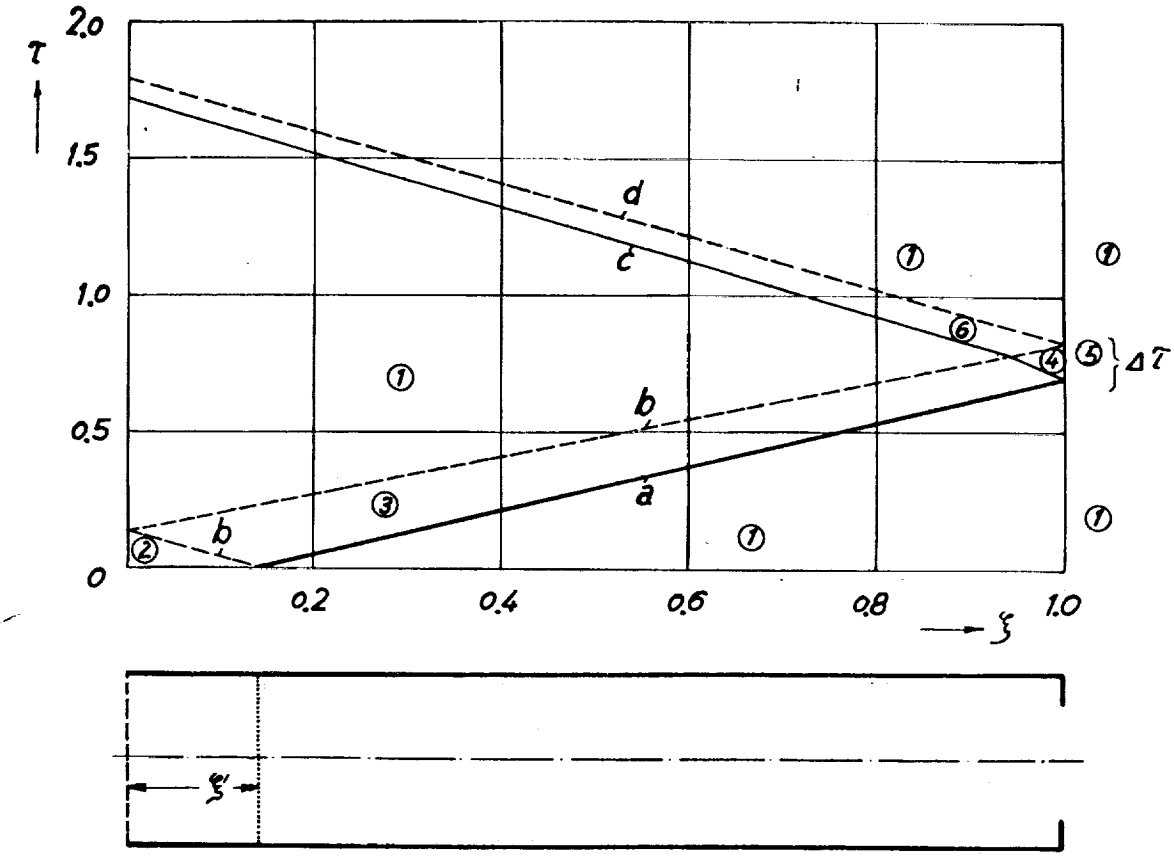

Figure 16. - Wave propagation in the jet tube. $F_E/F_R = 0.4$; form D.

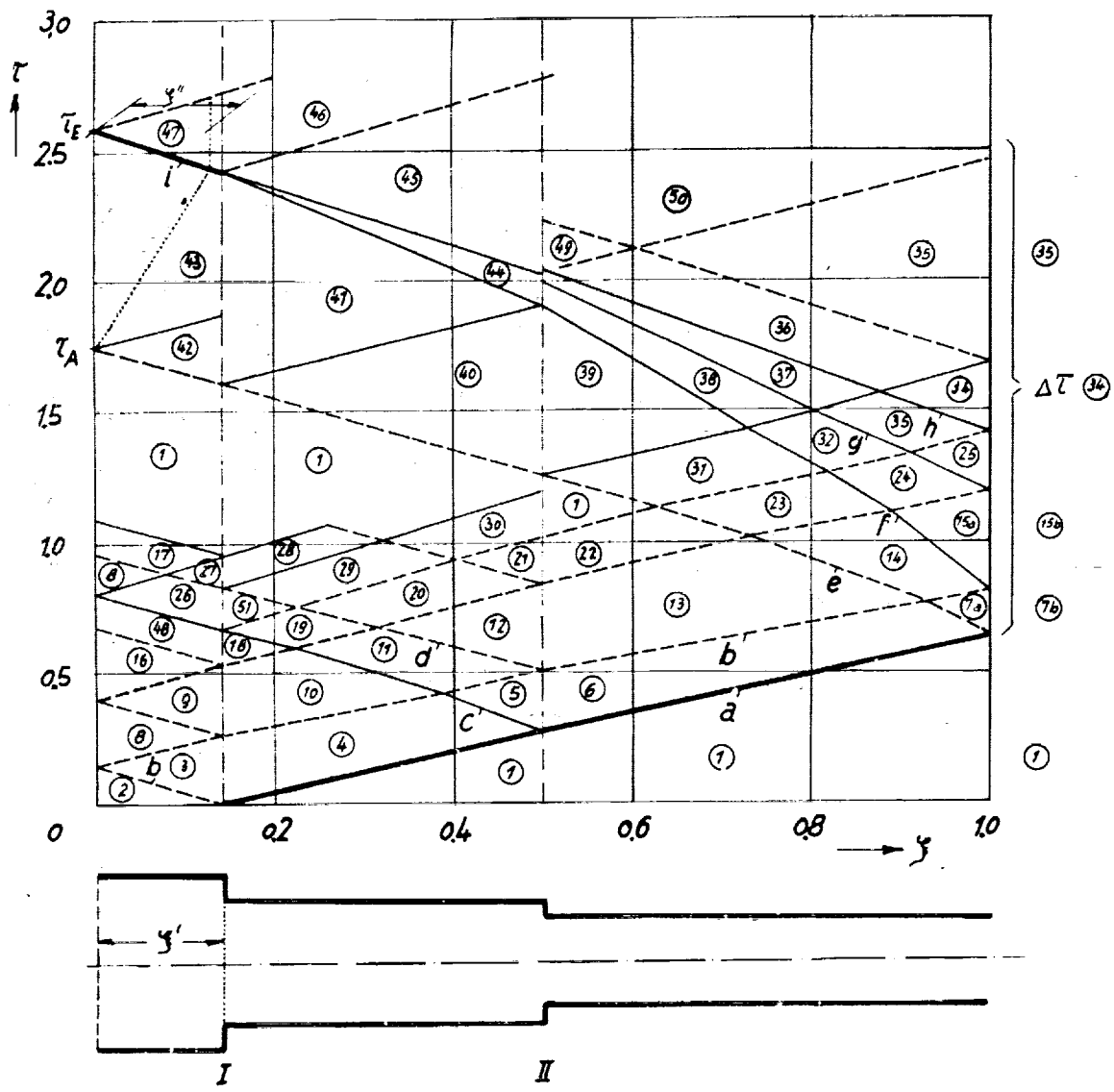

Figure 17. - Wave propagation in the jet tube. $F_E/F_R = 0.4$; form E.

621

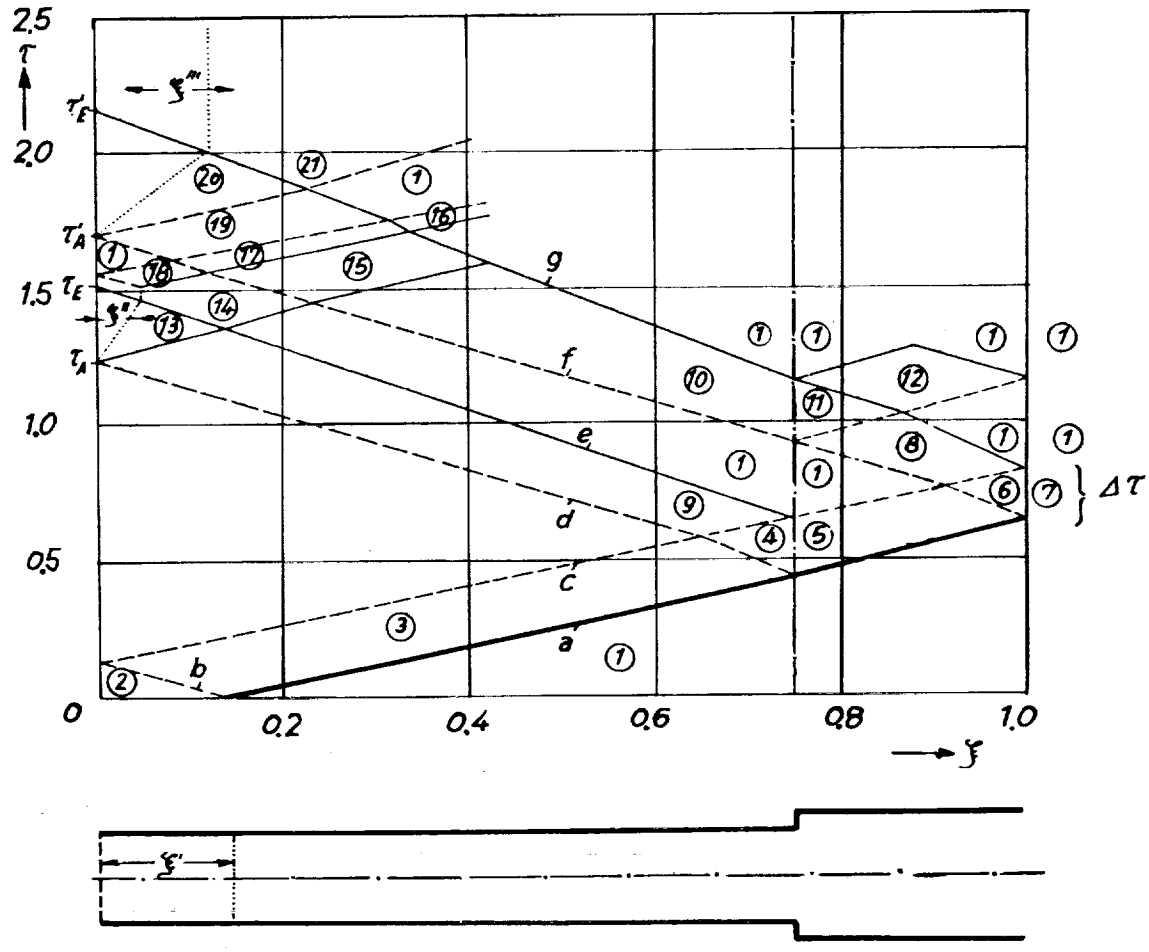

Figure 18. - Wave propagation in the jet tube. $F_E/F_R = 0.4$; form F.

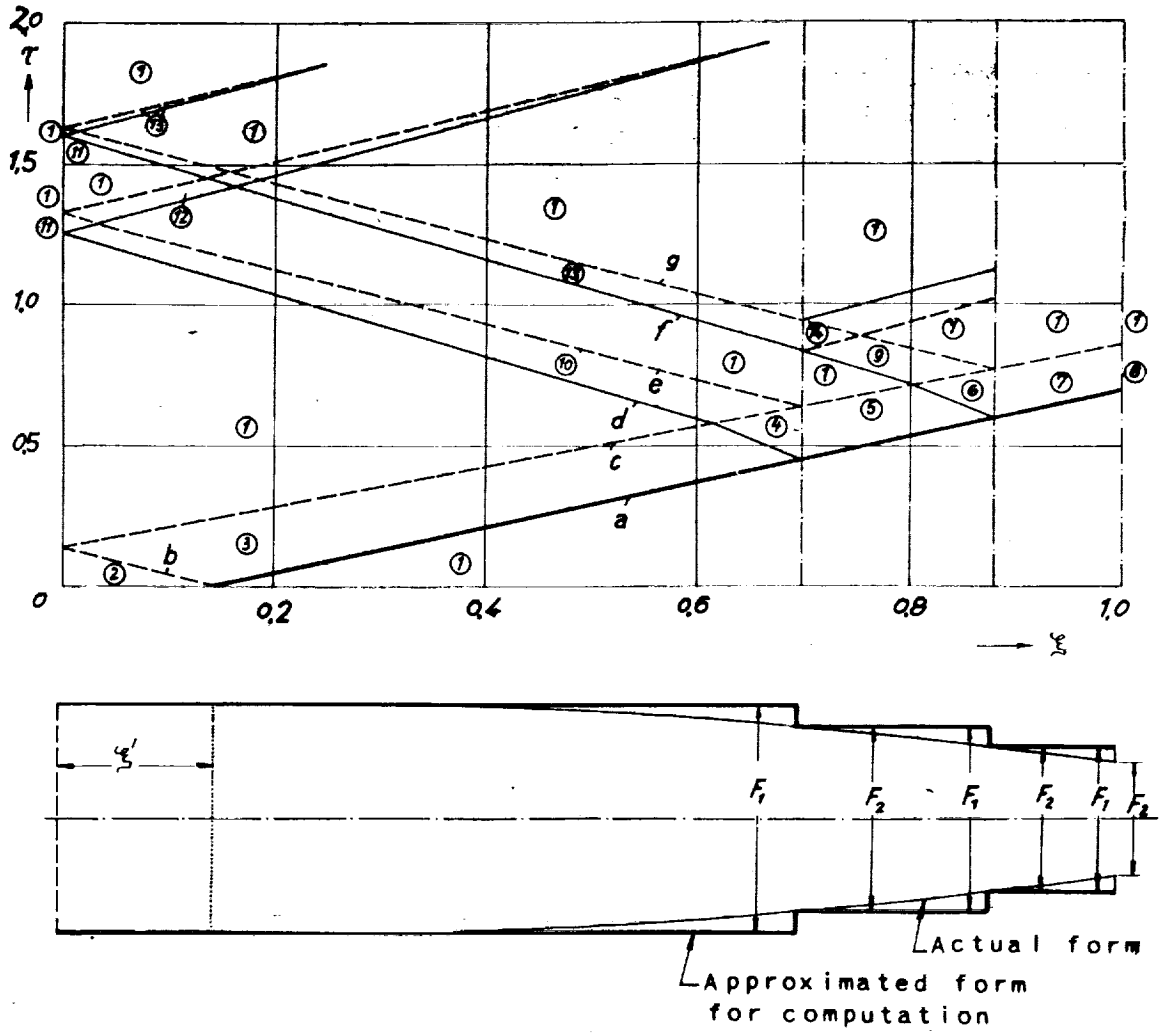

Figure 19. - Wave propagation in the Argus VSR9z jet tube. $F_E/F_R = 0.4$.

621

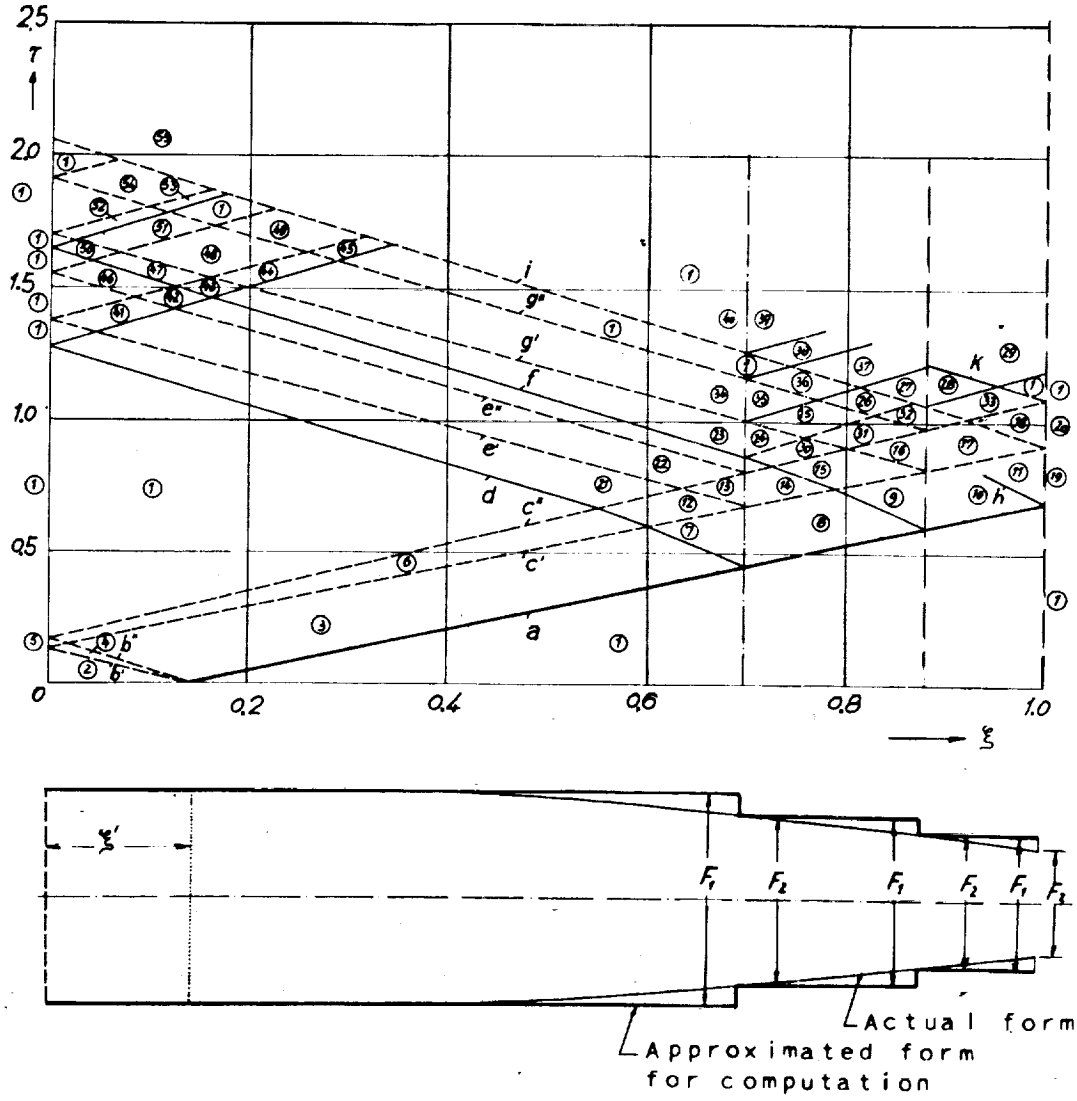

Figure 20. - Wave propagation in the Argus VSR9z jet tube. $F_E/F_R = 0.4$. (Closer approximation than in fig. 19.)

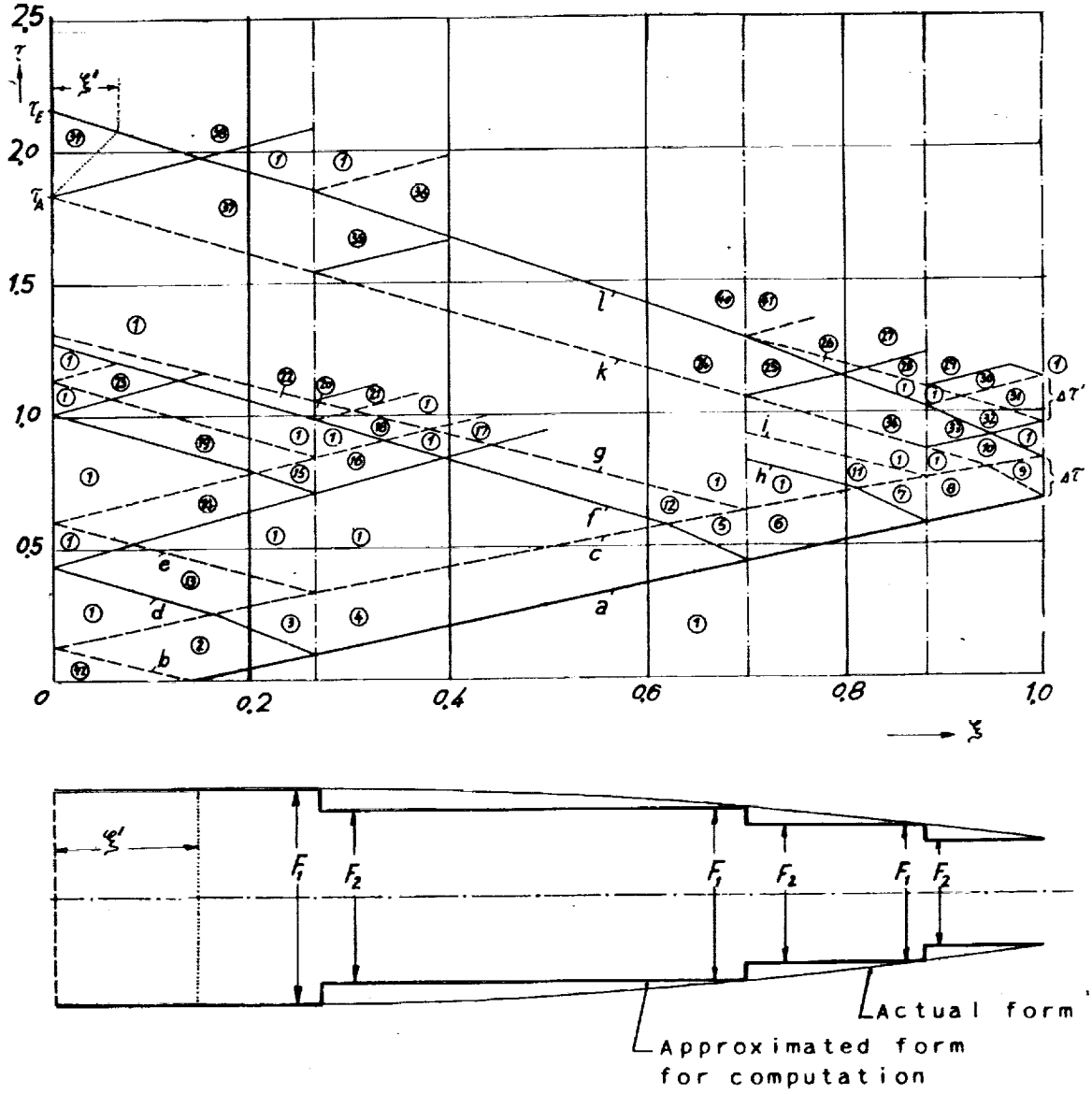

Figure 21. - Wave propagation in the Argus VSR9z jet tube. $F_E/F_R = 0.4$.

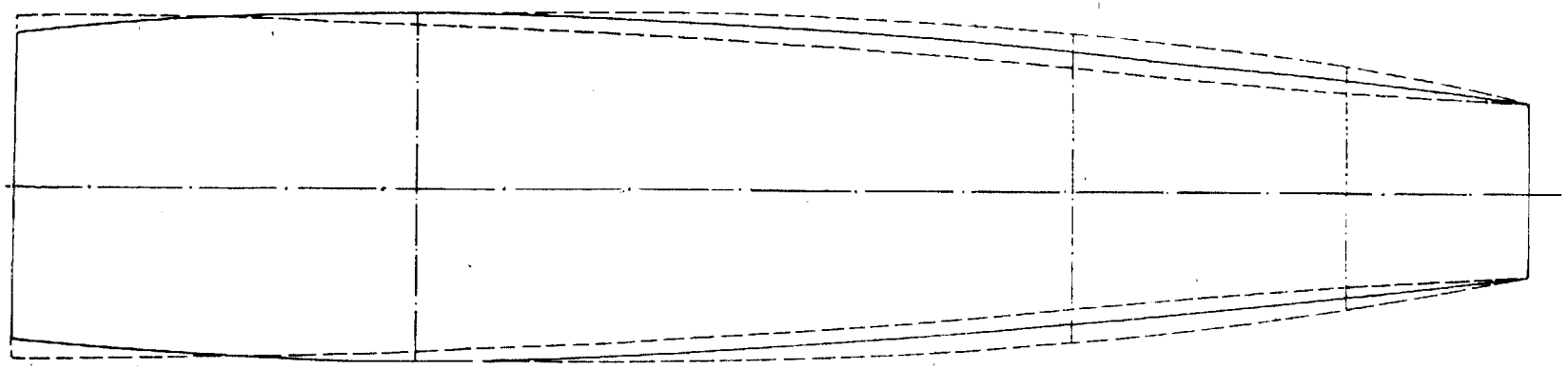

– – – – – – – Mean curves for two step-curves as approximations

——————— Actual curves

Figure 22. - Longitudinal section through VSR9z.

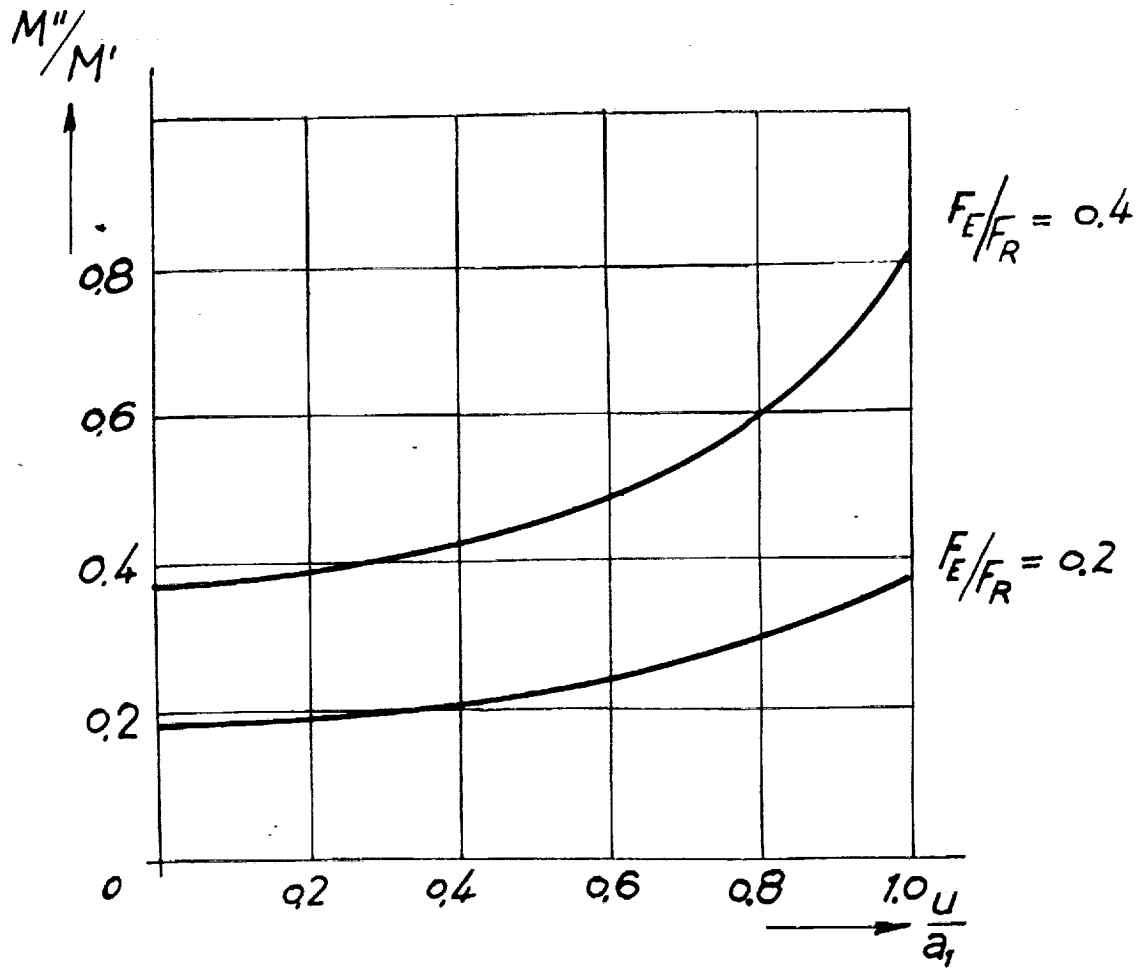

Figure 23. - Ratio of newly indrawn quantity of fresh charge M'' to quantity originally present M' as function of flight speed u.

621

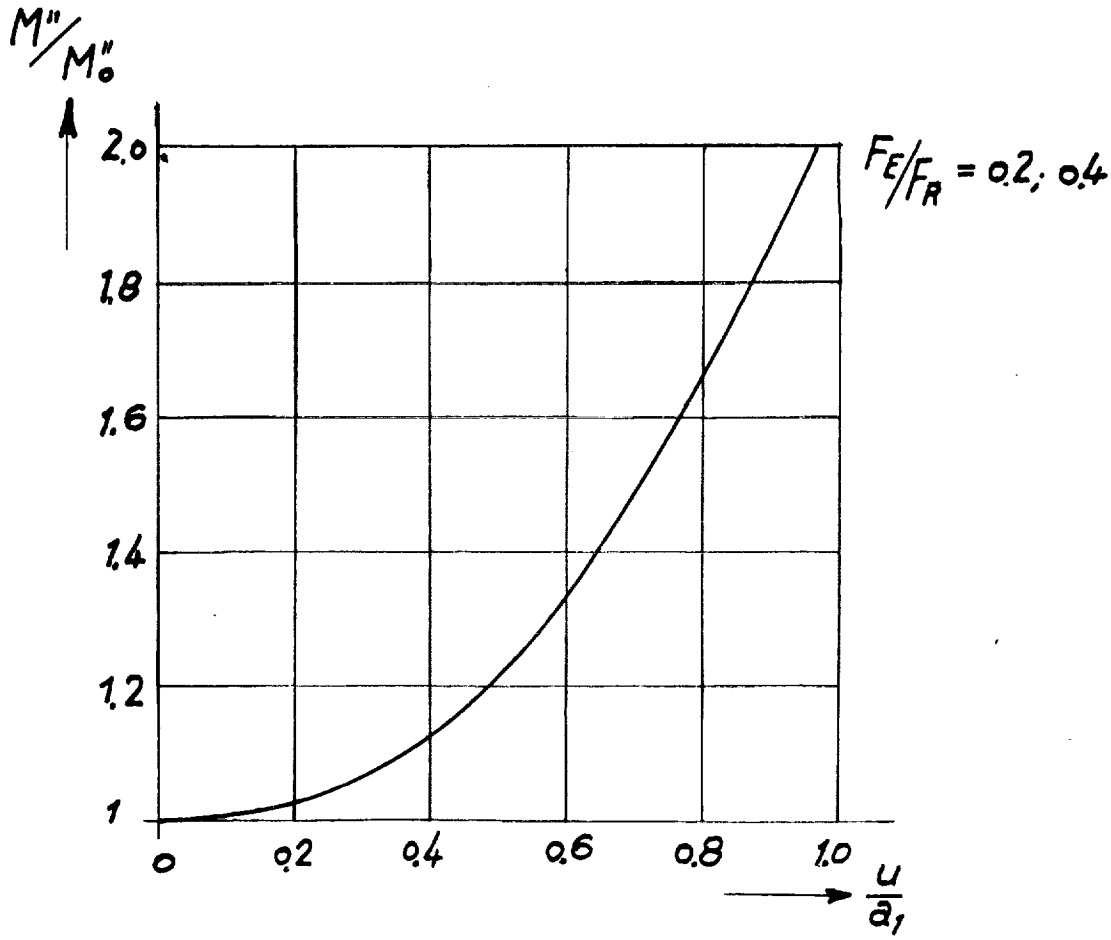

Figure 24. - Ratio of newly indrawn quantity of fresh charge M" to indrawn quantity M''_o when u = 0 as function of flight speed u.

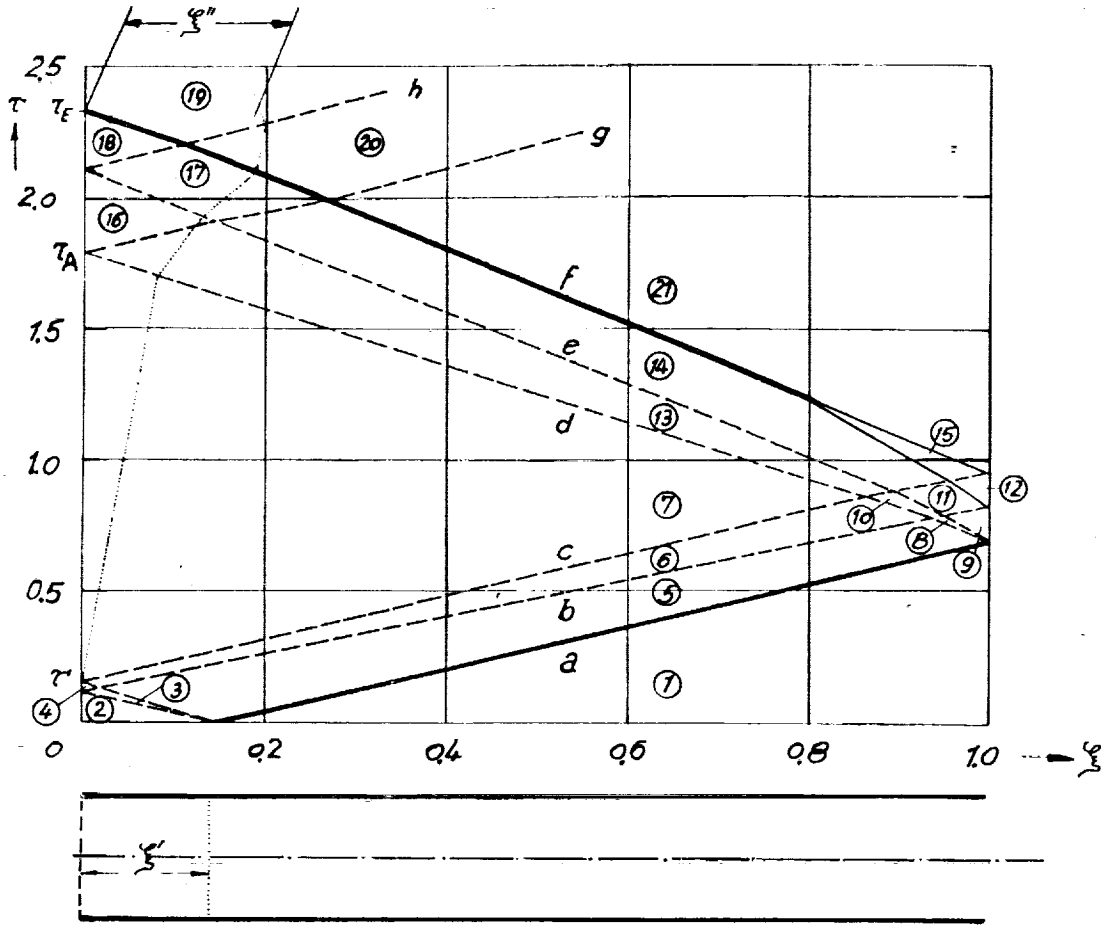

Figure 25. – Wave propagation in jet tube in the case of leakiness in the valves. $F_E/F_R = 0.2$; leakiness 50 percent, that is $\Delta F_E/F_R = 0.1$; flight speed = 0.64 of velocity of sound.

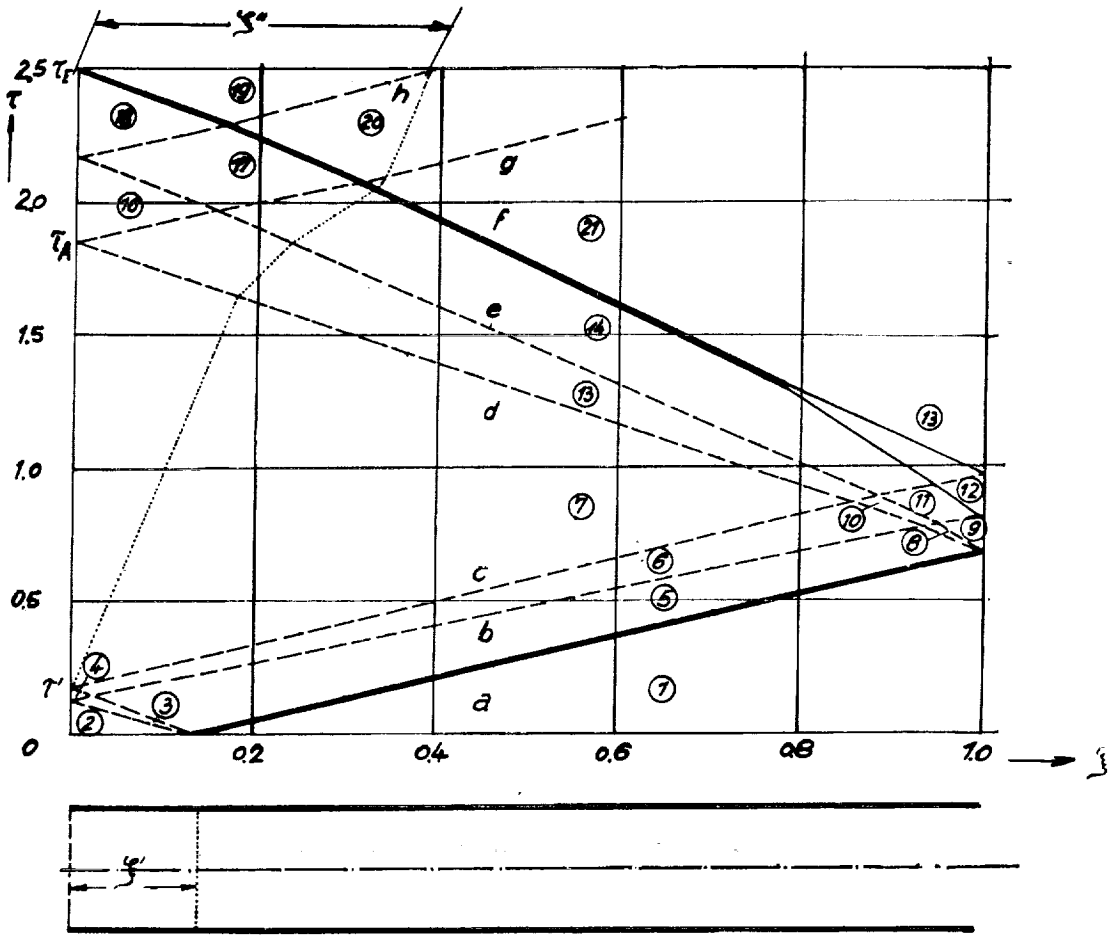

Figure 26. - Wave propagation in jet tube in the case of leakiness in the valves. $F_E/F_R = 0.2$; leakiness, 100 percent, that is $\Delta F_E/F_R = 0.2$; flight speed = 0.64 of velocity of sound.

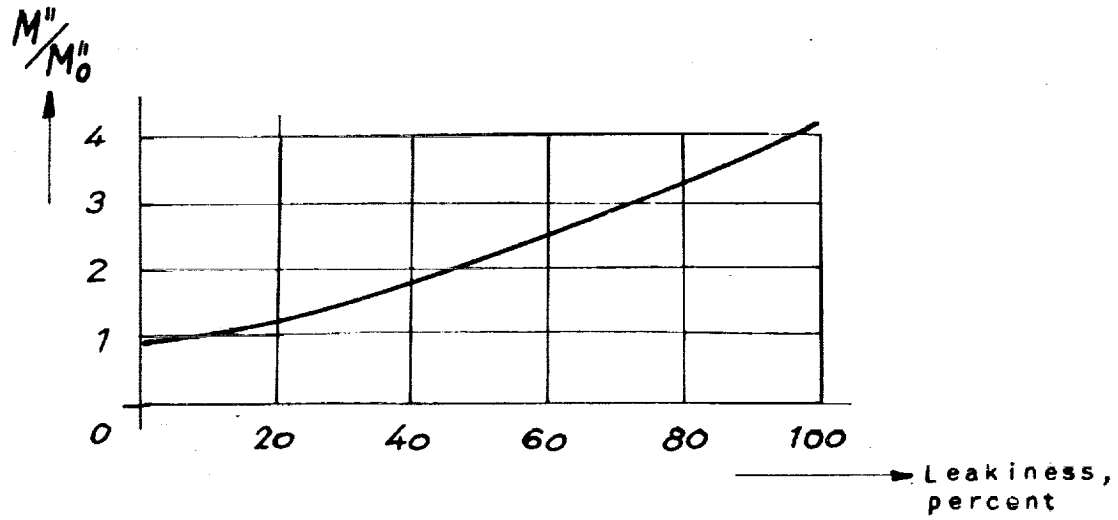

Figure 27. - Ratio of quantity of newly indrawn gas M" to quantity drawn in with zero leakiness $M"_o$ plotted against leakiness in percentage of fully opened valve cross section F_E/F_R = 0.2. Flight speed = 0.64 of velocity of sound.

621

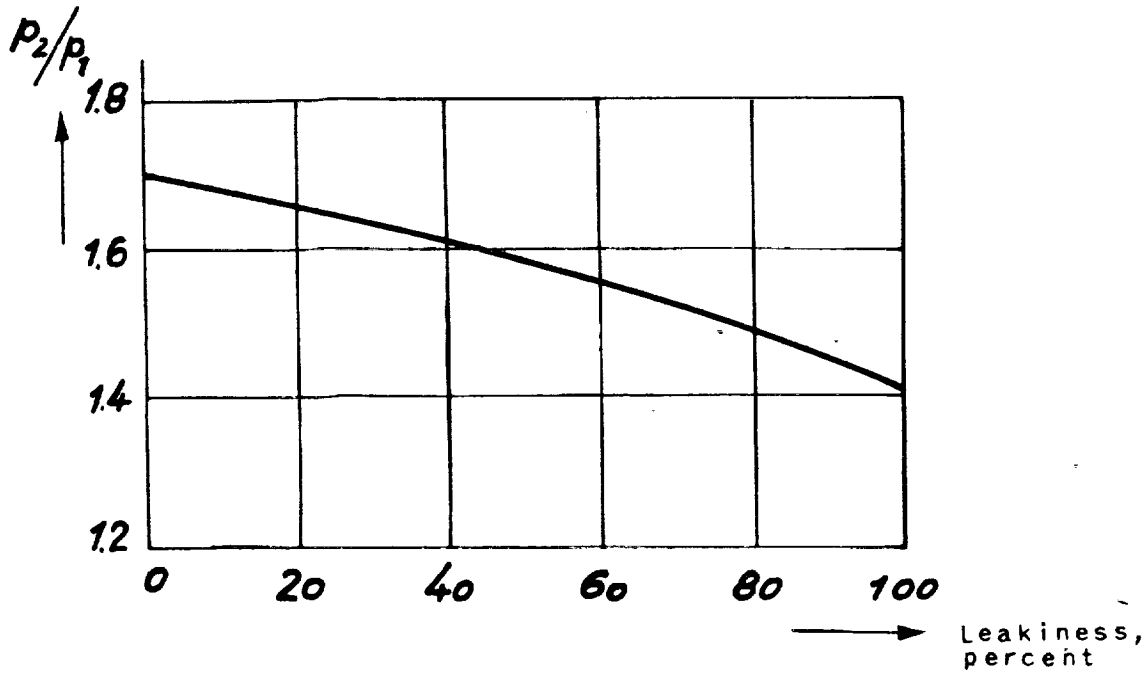

Figure 28. - Pressure ratio in returning (igniting) compression shock f plotted against leakiness. (Same conditions as in fig. 27.)

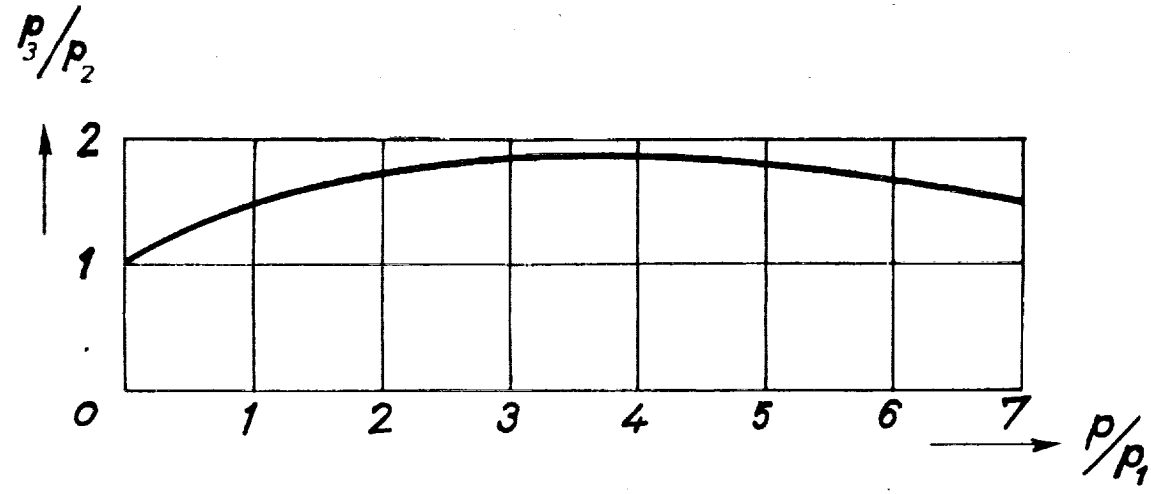

Pressure ratio p_3/p_2 in reflected shock 3 (p_3 before and p_2 after the shock) plotted against combustion pressure.

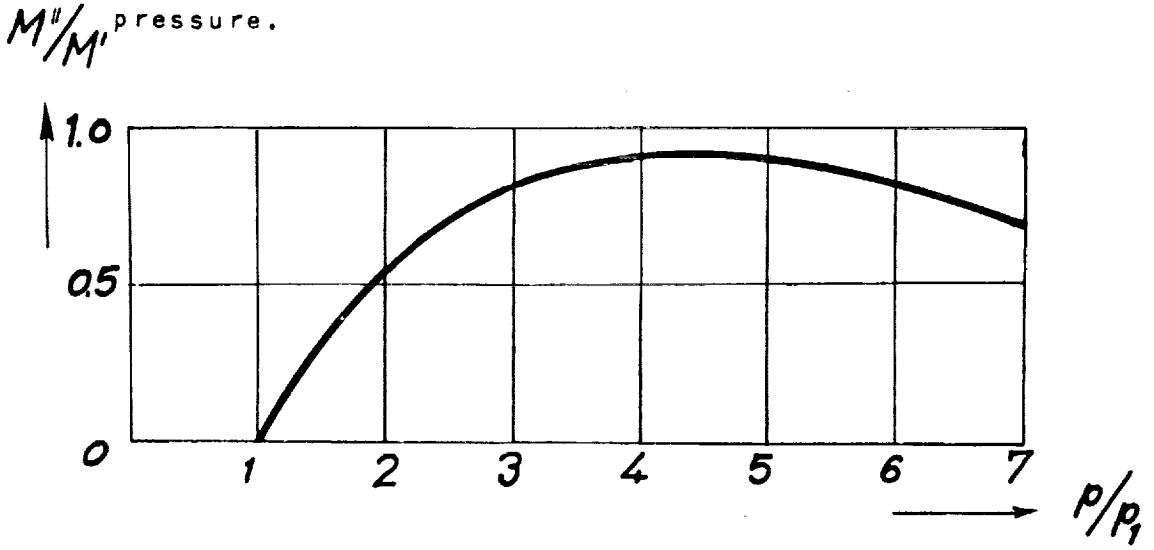

Ratio of newly indrawn quantity of fresh charge M" to quantity originally present M' plotted against combustion pressure.

Figure 29. - Influence of combustion pressure p.

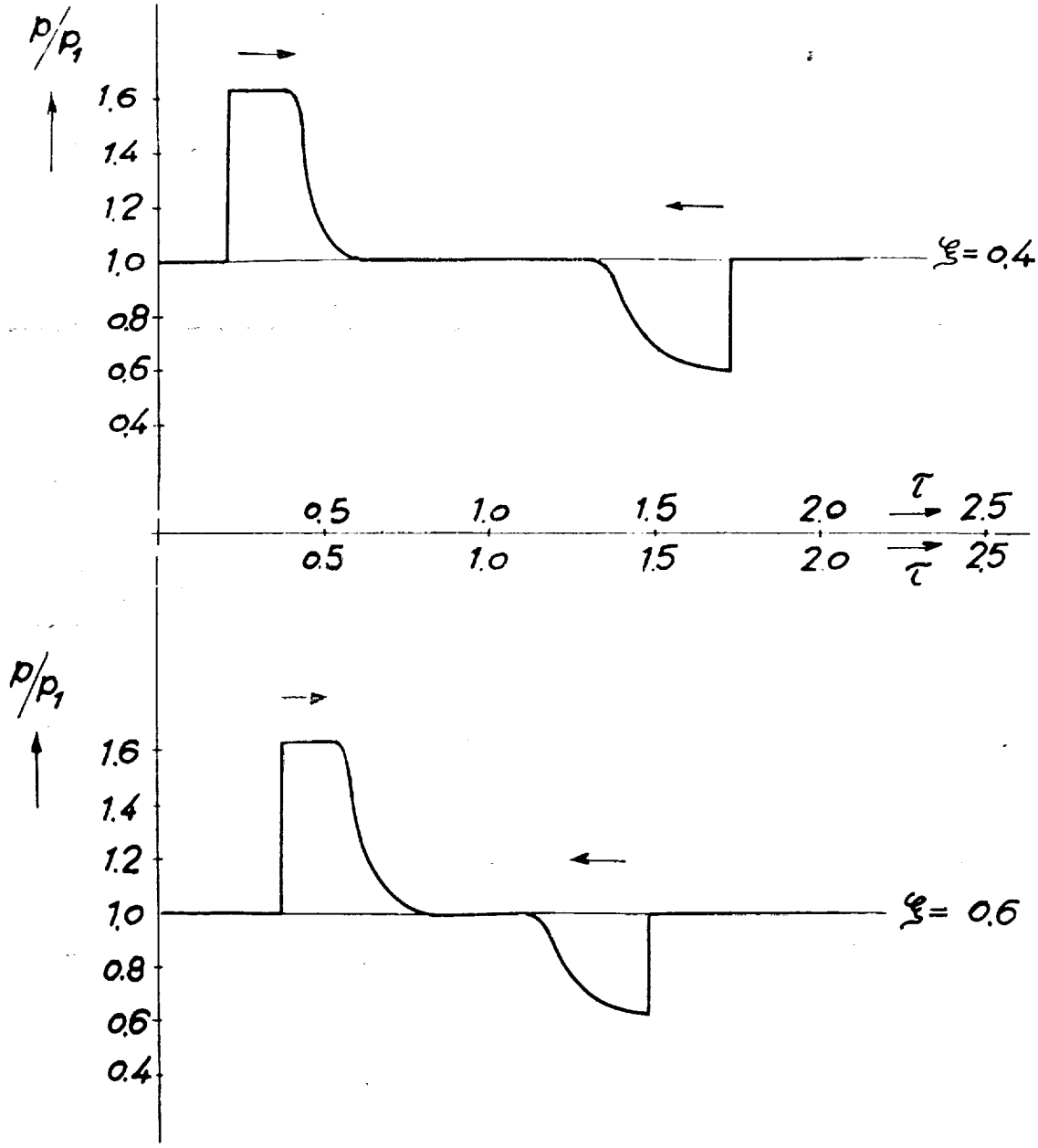

→ Outward-traveling wave (+ξ direction)

← Inward-traveling wave (-ξ direction)

Figure 30. - Variation of pressure with time at cross sections. $\xi = 0.4$; $\xi = 0.6$; form A (cylindrical tube). (See fig. 11.)

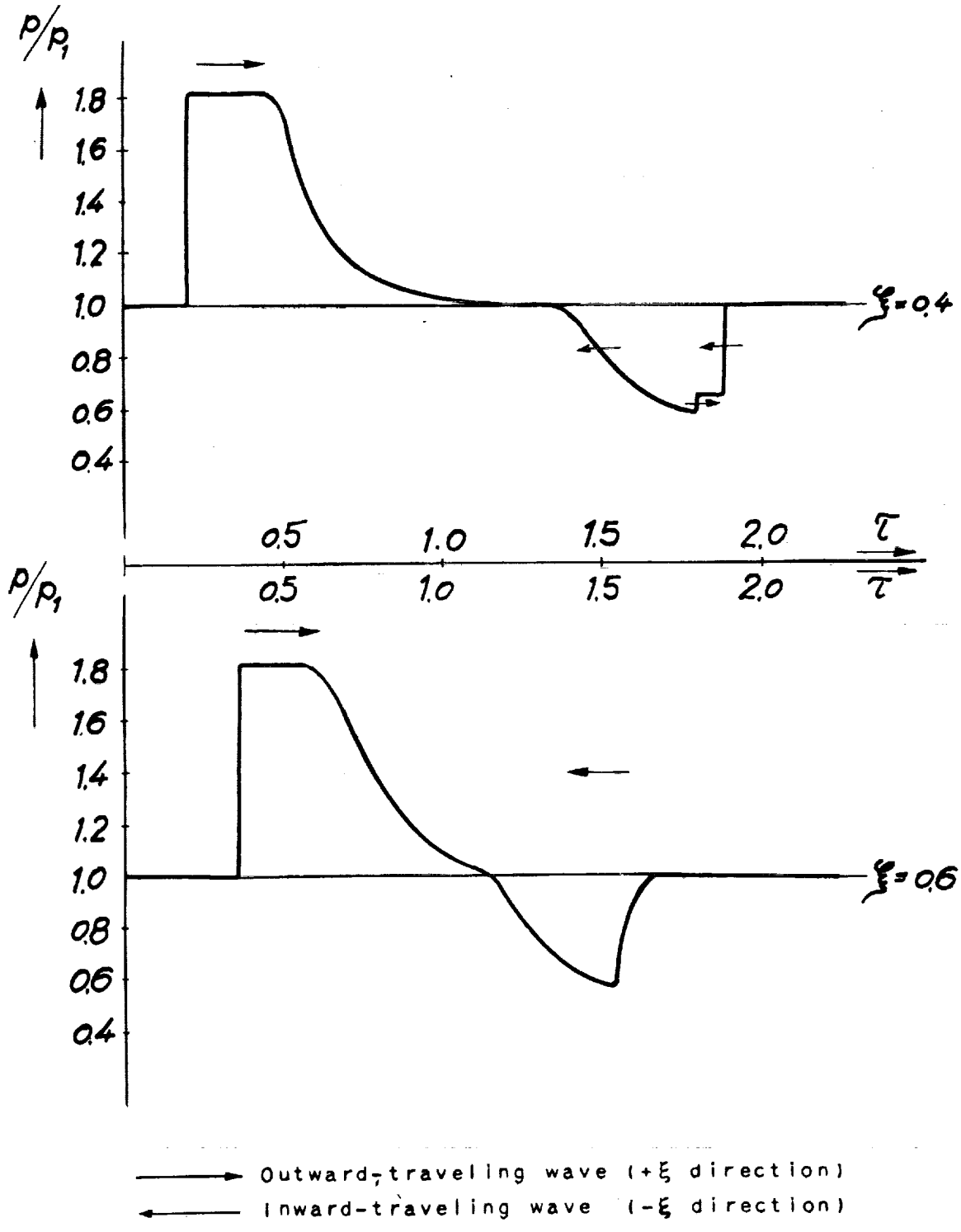

Figure 31. - Variation of pressure with time at cross sections. $\xi = 0.4$; $\xi = 0.6$; form B. (See fig. 13.)

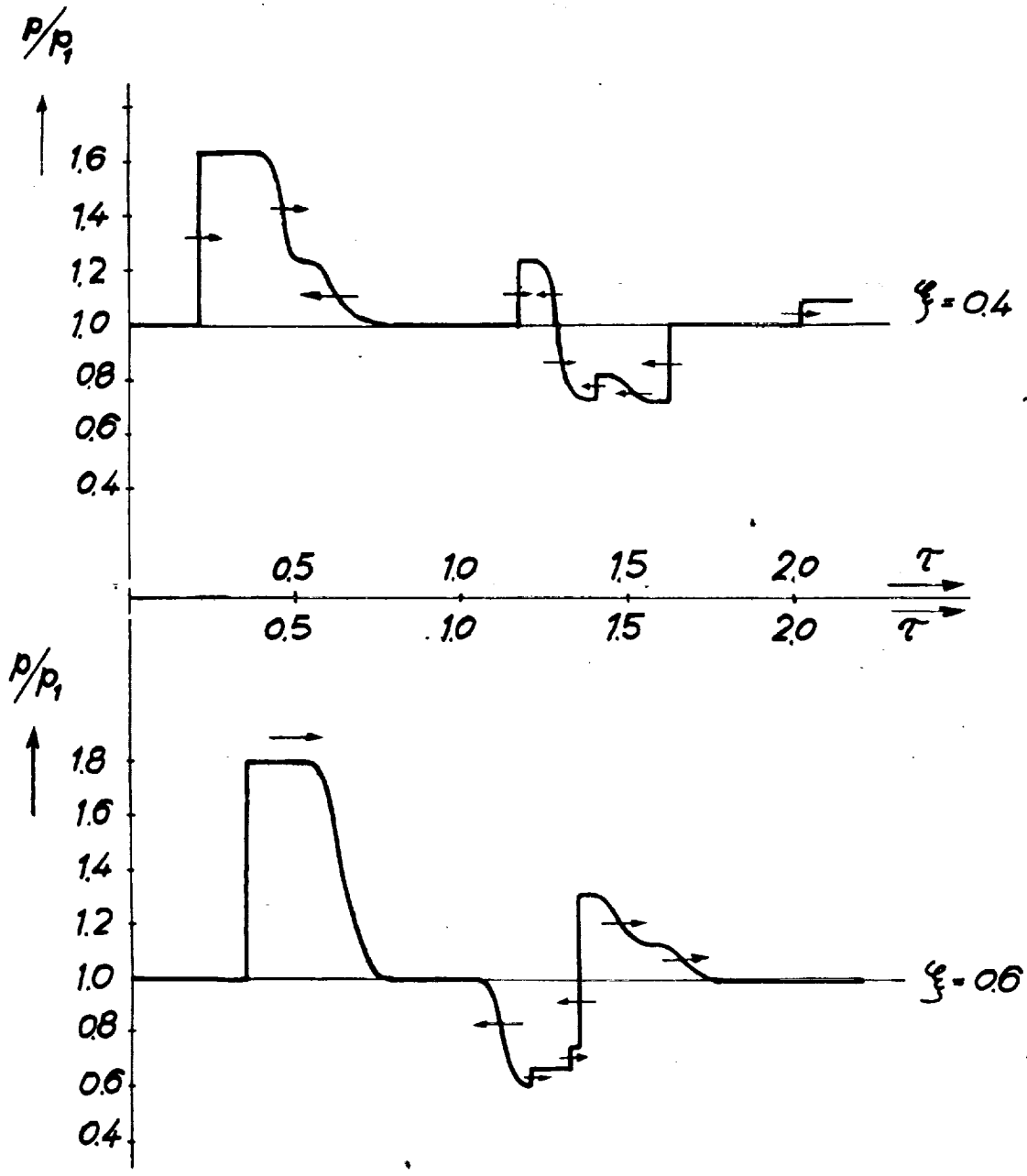

Figure 32. - Variation of pressure with time at cross sections. $\xi = 0.4$; $\xi = 0.6$; form C (See fig. 13.)

GAS-DYNAMIC INVESTIGATIONS OF THE PULSE-JET TUBE

PART II

SUMMARY

This investigation will account for the important practical observation made by Paul Schmidt that the ratio of the effective valve cross-sectional area to the tube cross section may not be of any random magnitude and will explain why at too great flight speeds the jet tube ceases to operate. Chemical and thermodynamic processes (for example, constituents or mode of fuel-air-mixture formation or heat losses) are unimportant in this regard.

INTRODUCTION

In Part I the jet tube was investigated using the simplest possible assumption as to the initial condition, namely, that a compressed column of fresh charge suddenly expands. The simplification thus obtained permitted an elementary insight into the nonuniform gas motion, even in noncylindrical tubes. The investigation attributed the setting-off of the explosion to a compression shock wave reflected from the end of the tube and it was useful in that it enabled a prediction as to which tube forms that were aerodynamically desirable would also be capable of operating. It was shown that in tubes tapering toward the rear, the end portion of the tube must be cylindrical.

The investigations of Beckert and Sauer are based on very similar simplified initial conditions.

But the combustion does not take place suddenly; instead, it extends over a rather large part of the working cycle. The consequent variation of pressure with time will be investigated in the cylindrical tube. Because nothing is known of the combustion as a function of the condition values, an experimentally determined value shall be used for the increase of pressure due to combustion; and the simplified assumption shall be made that the change of state takes place adiabatically and simultaneously along the whole column of fresh charge. This assumption presupposes combustion taking place in that manner. In actual fact, the combustion takes place not solely from the end cross section of the column of fresh charge but from the outside inwardly along its whole length due to the continuous presence of burning remnants of the previous charge.

Accordingly for the purposes of this investigation, the only effect of the fuel is the production of a change of state of the fresh charge. The influence of its mass upon the motion will be neglected.

The exhaust gases are assumed to have the same specific heats as the fresh charge and their state is assumed to lie on the same adiabatic curve as that of the fresh charge.

These assumptions imply that in the jet tube a homogeneous gas initially exists throughout under uniform pressure, upon which, confined in a limited space, an adiabatic change of condition is externally imposed.

Comparison with Paul Schmidt's experimental results will show whether a gas flow corresponding to reality arises under the premises thus assumed.

This investigation will be carried out using the Riemann theory of nonuniform gas flow, according to which the gas flow is determined by the propagation of pressure waves. The propagation will be graphically represented in a time-distance diagram. The method of approximation (reference 1) to be used for this purpose has been described in Part I and here is assumed to be familiar.

GAS FLOW DURING AN EXTERNALLY CAUSED CHANGE OF PRESSURE

With an increase of pressure in the column of fresh charge there arises a pressure difference as compared to the exhaust gases adjoining the rear face of this column. This pressure difference results in a movement of expansion, which is transmitted to the exhaust-gas column as condensation waves and to the fresh-charge column as rarefaction waves, in the manner indicated in the time-distance diagram of figure 1'. The assumptions that the change of state is isentropic and that the entropies of fresh charge and exhaust gases are the same lead to the further assumption that these waves are produced in pairs consisting of a condensation wave and a rarefaction wave of equal strength.

With this method of approximation, only a few of the continuous series of waves that are transmitted shall be followed; also as an approximation, constant gas and sound velocities between them shall be assumed. Likewise, the continuous externally imposed increase in pressure will be approximated by separate small jumps, the position and magnitude of which will be determined by the experimentally observed sequence of pressure variations. It is assumed that these

abrupt changes take place simultaneously throughout the whole column of fresh charge. They are represented in figure 1' by solid horizontal lines.

With the definition of the manner which the externally imposed pressure varies with time, the simplest premises possible for its variation with the distance x shall be defined. Let the imposed pressure change be taken as uniform throughout the column of fresh charge. It is then obvious that this change will have no direct effect on the motion of the gas but only a later indirect effect caused by the successively generated waves that are transmitted from the end of the column of fresh charge. Pressure variations corresponding to the already existing waves remain; the waves do not change in strength but do change their rate of propagation because of the change in the velocity of sound.

In order to conduct the investigation, the relation is required between the change in gas velocity Δu and the change in velocity of sound Δa resulting from the wave

$$\Delta u = \pm \frac{2}{\kappa - 1} \Delta a$$

and the expression for the velocity of propagation of a wave

$$w = \pm a + u$$

The upper sign applies to a wave traveling in the +x direction; the lower, to one traveling in the -x direction.

COMPUTATION OF GAS MOVEMENT DUE TO GIVEN RISE IN PRESSURE IN COLUMN OF FRESH CHARGE

From pressure measurements on jet tubes, it is found that the pressure rise during combustion corresponds, for the purposes of this investigation, to an increase in the sonic velocity $\Delta a = 0.04 a_1$ in 1/15 the time required for a wave to traverse the jet tube with a sonic velocity a_1 of the atmosphere at rest. On this basis, the rise to the normal value of 2.5 times atmospheric pressure requires an interval of about 1/5 of the working cycle.

According to the observations of Paul Schmidt, the column of fresh charge extends for 1/7 the tube length. At the beginning of the first working cycle, the fresh-charge column is allowed to expand. Let the quantity of charge distributed through 1/7 of the

tube length be the proper quantity for continuous tube operation, the quantity that must be drawn in during each period. This fixes the maximum pressure during a cycle because that pressure substantially determines the quantity drawn in for the next period. Thus for the first cycle a maximum pressure of 5.5 times atmospheric and for the second cycle 3.5 times is obtained. The reason for the lower value for the second period is that a motion process already exists from the first period.

The ratio of maximum effective valve area to tube area is set at 0.4. The reflection of the waves at the valves has been explained in Part I. A rough allowance shall be made, however, for the mass and stiffness of the springs by assuming a gradual opening of the valves to their maximum stroke.

The initial phases of tube operation will be treated here rather than the ultimate oscillatory action because the Riemann theory refers to the initial phases. In view of the rather burdensome work involved, only the first two periods will be developed. The second period will give a sufficient idea of the essentials of the ultimate oscillatory action.

The wave propagation in the time-distance diagram has been constructed in figures 7' to 11'. Here the condition of motion and state of the gas at all tube cross sections and at all times may be found and along x = constant and t = constant lines the time sequence of pressure at a given cross section and the distribution of pressure along the axis of the tube at a given time may be read. As coordinates, take dimensionless time $\tau = t\frac{a_1}{l}$ and dimensionless distance $\xi = x/l$, in which l = tube length. The slope of a line of propagation measured from the τ-axis is thus a velocity made dimensionless by dividing it by a_1, the sonic velocity of the initial state of rest. The values of the states existing at each point are shown in figures 7' to 11'. [NACA comment: The pair of numbers shown in each area of figures 7' to 11' are the values of a/a_1 (upper) and u/a_1 (lower), respectively. The pressure may be calculated from the relation $p/p_1 = (a/a_1)^{2\kappa/(\kappa-1)}$.]

In order to permit a better over-all view, figure 2' gives a summary of the wave propagation that is constructed in detail in figures 7' to 11'. In figure 2', pressures above and below atmospheric are indicated by + and - signs, and the direction of the flow by arrows.

The condensation waves A' and A" (fig. 2'), which arise from the combustion in the first and second cycles, initiate an outflow from the end of the tube at greater than atmospheric pressure and at the velocity of sound. Consequently, the subsequent rarefaction waves B' and B" are reflected as rarefaction waves C' and C" until they have liquidated the excess pressure. The still later rarefaction waves D' and D" are reflected as condensation waves E' and E"; they produce a condition of atmospheric rest. This condition exists in the regions designated I.

At the inlet end, the waves C' and C" initiate the intake period. When the first wave arrives, the valves are still closed. From that moment on, due to their inertia, they gradually open. The first waves are consequently reflected as the rarefaction waves F' and F"; the last waves are reflected as the condensation waves G' in the first cycle and not reflected at all in the second.

The first cycle influences the second cycle through waves E', F', and G'. The fresh charge drawn in during the first cycle is compressed and, as indicated in Part I, is also ignited by waves E', because obviously no other phenomenon exists that might serve to set off the explosion. The second cycle begins with this ignition.

Wave G' combines with the pressure waves originating in the second explosion, thereby reinforcing them.

The rarefaction waves F' are reflected at the end of the tube as condensation waves H' and produce at that point inward flow with a maximum gas velocity of $u/a_1 = 0.18$. The boundary of the inflowing air is shown by a finely dotted line. This air eventually occupies 1/8 of the tube. This phenomenon of inward flow at the exhaust end of the tube was experimentally observed by Paul Schmidt and termed by him "intrusion of air." This phenomenon was considered unimportant and hence not treated in Part I of this report because its occurrence was not so obvious on the basis of the simpler initial conditions assumed in Part I.

The effect of waves H' is to produce, following the combustion, a pressure higher than atmospheric at the inlet end, which exists until the arrival of rarefaction waves C". These waves C" initiate the second intake period.

Figure 3' shows the variation of pressure with time at the inlet end, as derived from the time-distance diagram.

COMPARISON WITH EXPERIMENTALLY OBSERVED RESULTS AND CONCLUSIONS

For comparison, figure 4' shows experimental results obtained by Paul Schmidt. It is apparent that the calculated pressure diagram (fig. 3') substantially agrees with his.

It is of especial interest that an explanation can now be made for the shoulder in the curve H in figure 4', which appears more or less markedly in all observations of pressure at the inlet end. It appears also in the pressure diagram that has been calculated (fig. 3') and is in fact produced by the waves H', which were originally reflected from the open valves. It is thus seen to be a phenomenon of valve operation. The stiffer the valves are and the more mass they have the more this shoulder will peak.

On the other hand the comparison shows that the combustion does not begin suddenly with a constant speed of burning, as has been here assumed for the sake of simplicity. The irregularities at the beginning of the experimentally observed pressure rise must be due to vibration of the valve flaps, which will be disregarded here.

In Part I, the occurrence of the condensation waves E was found as a criterion of the tube operability, from which it was evident that tubes with a constriction at the exhaust end are not operable. A second criterion of operability now appears, one that simply expresses the observation of Paul Schmidt that operability is affected by the opening ratio of the valves, that is, the ratio of maximum effective open cross-sectional area of the valves to the cross-sectional area of the tube. In other words, with too great an opening ratio the tube will not operate.

The explanation for this is found in figure 2'. If the opening ratio is too great, scarcely any of the waves reflected at the valves will be rarefaction waves F' but instead predominantly condensation waves G'. The reflected waves H' are then not condensation but rarefaction waves. This means that the fresh charge will flow in at higher pressure and in greater quantity and the pressure level will thus be raised; but on the other hand, when the reflection of wave H' takes place at the open end of the tube an inflow (rebound), or as Paul Schmidt calls it as intrusion of air, will not occur but instead, due to the reversed character of the waves, a premature outflow will be initiated, namely, before the compression shock wave A" starts the exhaust process. The inflow of fresh charge thus has the effect of a weak intermediate explosion, that is, it creates a condensation wave analogous to G' traveling toward the open end of the tube. But the wave corresponding to H' consequently reflected from the end of the tube is now a rarefaction wave that weakens the explosion.

At the correct smaller valve-opening ratio there are, on the contrary as in figure 2', predominantly rarefaction waves F'. By reflection at the end of the tube, they give rise to the condensation wave H', which produces the intrusion of air and strengthens the explosion. Thus it may be seen that the pressure loss in the valves must be at least so great that the indrawn fresh charge has a pressure lower than that of the exhaust gas in the tube.

It might also be said, that when the valve-opening ratio is too great, the combustion creates too little pressure because it must instead produce volume to maintain the flow through the tube initiated by H'. The combustion thus continues the process that took place due to the open valves, namely, displacement of volume. The limiting case of combustion at constant pressure is approached. The tube is not operable in that case because a certain progressive change of pressure is necessary in order that enough fresh charge may be drawn in for the next period.

It is now also seen that the two requirements stated by Paul Schmidt, namely, not too great a valve-opening ratio and intrusion of air, are mutually interdependent; for it has been learned that with too great a valve-opening ratio the process of continuous flow through the tube is too predominant over the oscillatory process. For the development of sufficient pressure during the explosion, a back-flow at the open end, that is, intrusion of air, is necessary.

INFLUENCE OF FLIGHT SPEED ON OPERABILITY

In the case of the jet tube in flight, the level of pressure on the valves is increased by the amount of the dynamic pressure, as compared with the case of the fixed jet tube. At a sufficiently high flight speed, the increase is so great that the pressure of the indrawn fresh charge is not lower than the exhaust-gas pressure in the tube and the same phenomenon appears as in the case of a too great valve-opening ratio. Thus at a certain flight speed, the tube will cease to be operable for the same reasons as in the case of a too great valve-opening ratio.

These operating limits should be of more significance than those computed by Beckert from the limits of combustion set by too lean and too rich fuel mixtures because the combustion limits are quite broad for the range of atmospheric conditions that will be encountered and may easily be influenced by modifications of design.

In addition to this previously described injurious effect of flight speed, there is the effect pointed out in Part I, namely, that with increasing flight speed the compression shock that sets off the explosion also becomes weaker, assuming the valve-opening ratio is kept constant.

SHIFTING OPERATING LIMITS TO PERMIT HIGHER FLIGHT SPEEDS

An extension of the operating limits would seem to be possible through automatic regulation of the valve-opening area in accordance with flight speed because a reduction in the opening ratio with increasing flight speed would fulfill the requirement of a sufficiently great pressure loss in the valves. However, it must also be made sure that a sufficient quantity of fresh charge is drawn in. This consideration sets the limit to the possibilities of opening-ratio regulation. In this connection, figure 23 of Part I, which is duplicated as figure 5' in this part, shows that with constant opening ratio increasing flight speed has little effect on the indrawn quantity of fresh charge up to a speed of 0.4 of the velocity of sound; after this point the effect is more marked. The regulating mechanisms therefore ought not to be operative until the higher flight speeds are attained. Figure 5' also gives a basis for estimating the possible scope of the regulation. At a flight speed of 0.8 of the velocity of sound, the reduction in the opening ratio ought to be about 25 percent.

Another simpler possibility is suggested in figure 6'. The full effect of the impact pressure is prevented by means of a cap in front of the tube. This cap will also reduce the flow resistance. The cap can be so formed that approximately atmospheric pressure will be attained at the annular slit where the fresh charge enters, regardless of flight speed. The introduction of air through the slit must, of course, be so arranged that turning losses are avoided.

REDUCTION OF INTERNAL-FLOW RESISTANCE

It may be asked whether it is possible to induce the oscillatory process by means other than valves with high flow resistance. One possibility would appear to be the positive mechanical regulation of the inlet area. It would then be possible to choose a relatively greater opening ratio maintained over a shorter time, rather than a smaller opening ratio operative for a relatively long time. On the one hand, the flow losses would then be less; and on the other, the opening of the valves could be made to occur as late as possible and

with maximum suddenness. Late opening would produce strong rarefaction waves F' because the valves would still be closed when the first waves C' struck them; and sudden opening would result in strong condensation waves G'. Both these effects would strengthen the subsequent explosion and thereby increase the thrust.

SUMMARY

By taking into account the course of the development of pressure by combustion, a new insight has been obtained into the processes of motion within the jet tube, an insight that explains a number of empirical observations, namely: certain particulars of the sequence of pressure variations; the existence of an optimum valve-opening ratio; the occurrence of an intrusion of air; and the existence of a flight speed above which the jet tube ceases to operate.

At too great an opening ratio or at too great a flight speed, the continuous flow through the tube is too predominant over the oscillatory process to permit the occurrence of an explosion powerful enough to maintain continuous operation.

Certain possible means of making the operation of the jet tube more independent of the flight speed and of reducing the flow losses were proposed and discussed.

Translation by Edward S. Shafer,
National Advisory Committee
for Aeronautics.

REFERENCE

1. Schultz-Grunow, F.: Forsch. Ing.- Wes., Bd. 13, Heft 3, 1942, p. 125.

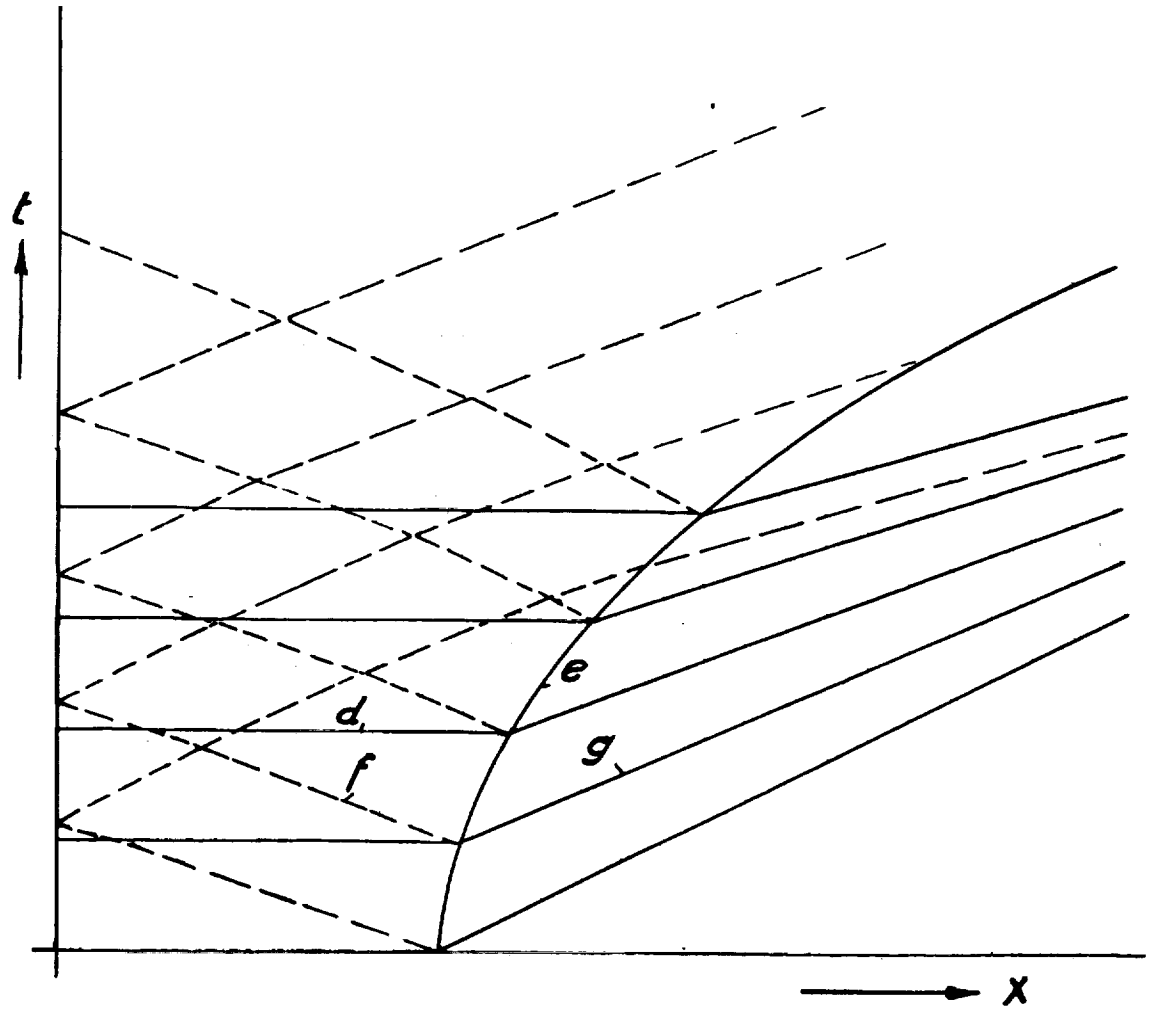

Figure 1'. - Expansion movement of column of fresh charge.

d Stages of pressure increase

e Line of propagation of fresh-charge boundary

f,g Waves of equal strength leaving fresh-charge boundary

—— Condensation waves

—— Rarefaction waves

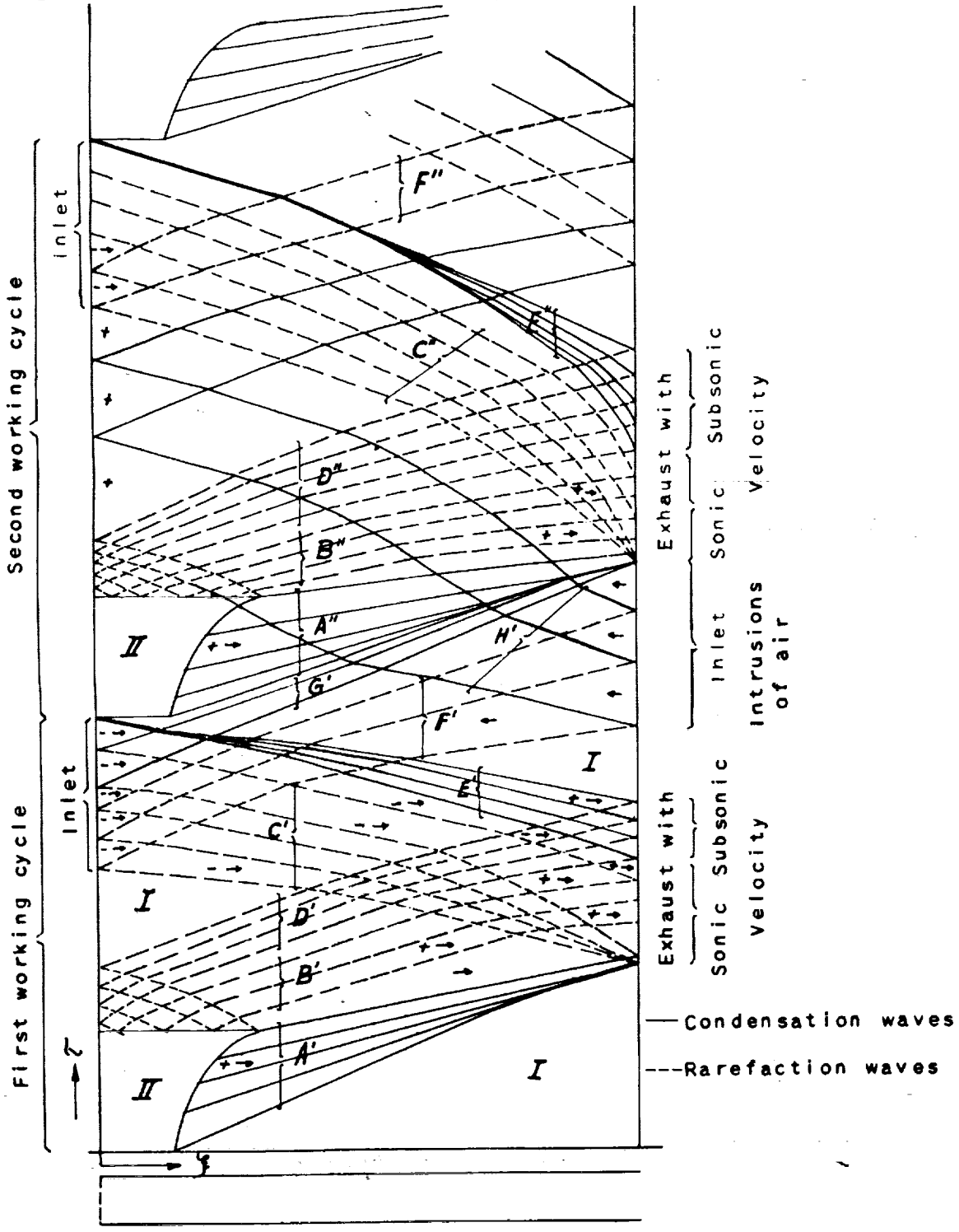

Figure 21. - Initial phases of operation of jet tube. Wave propagation in time-distance diagram. I, atmospheric condition of rest; II, combustion.

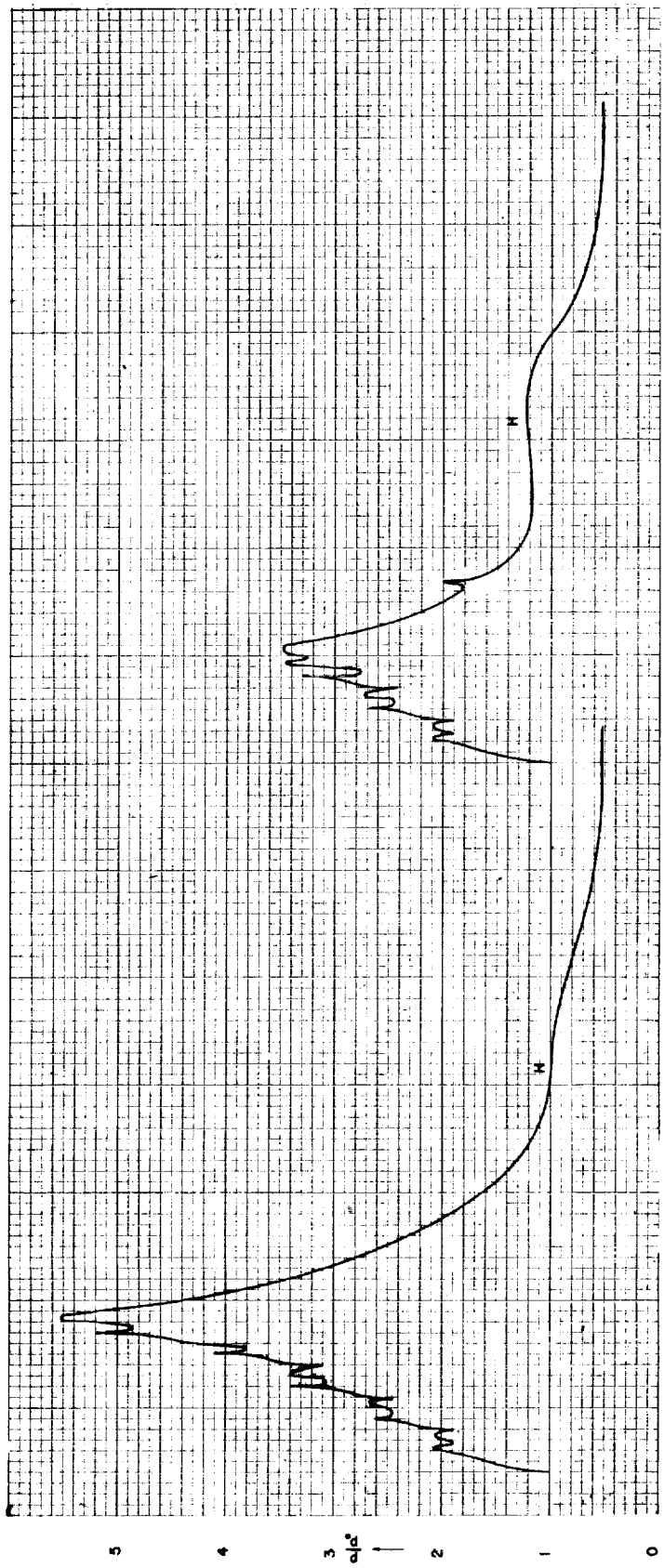

Figure 31. - Sequence of pressures at inlet end. (A $10\frac{1}{8}$ by 21-in. print of this figure is attached.)

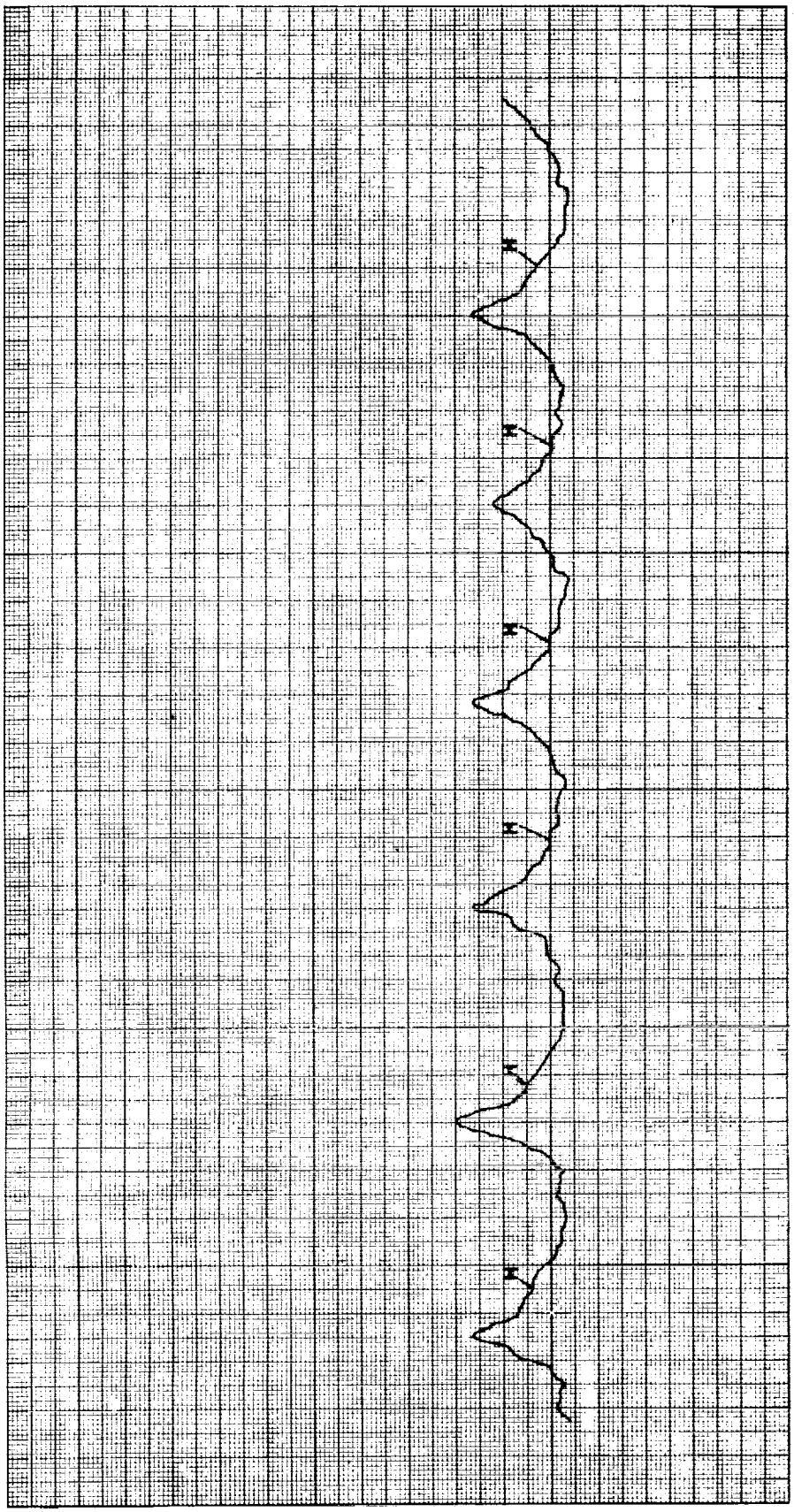

Figure 4'. - Experimentally observed sequence of pressures at inlet end obtained by Paul Schmidt.

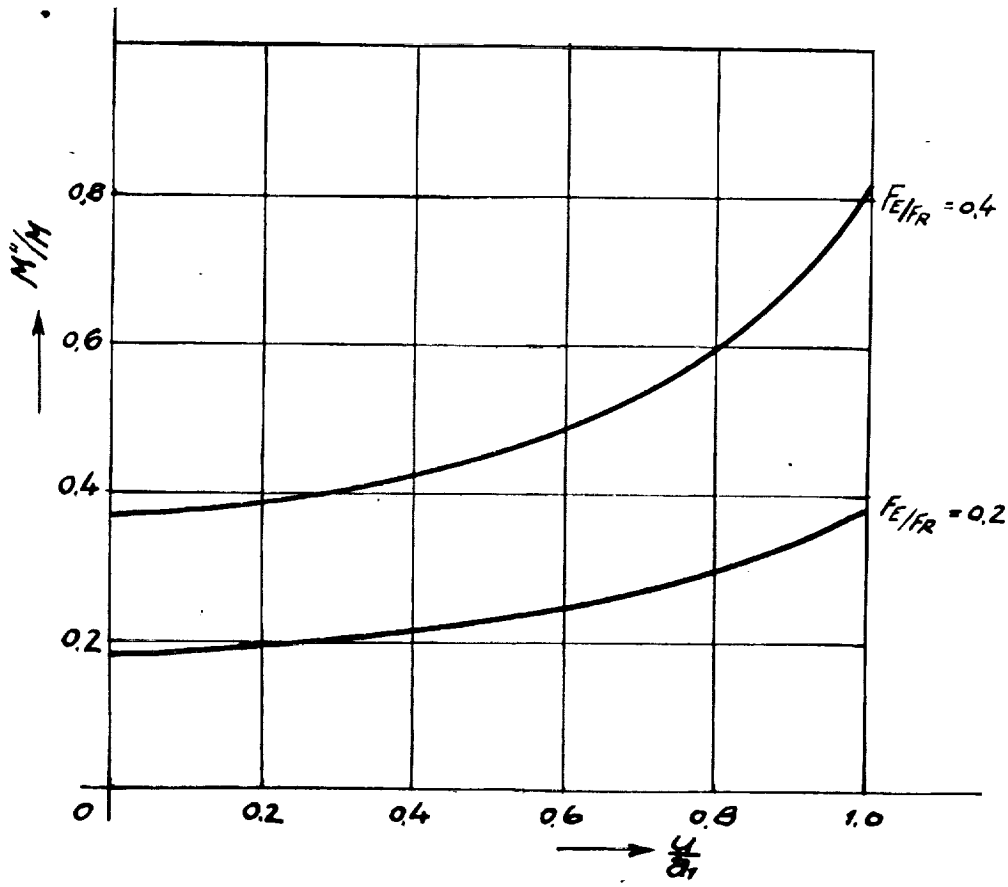

Figure 5'. - Ratio of newly indrawn quantity of fresh charge M'' to quantity originally present M' as function of flight speed u.

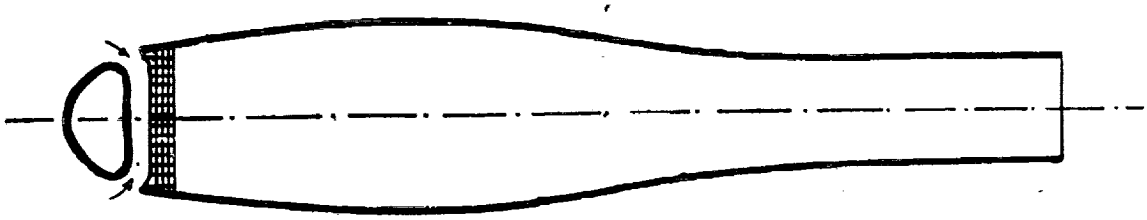

Figure 6'. - Jet tube having cap in front to reduce effect of impact pressure on valves.

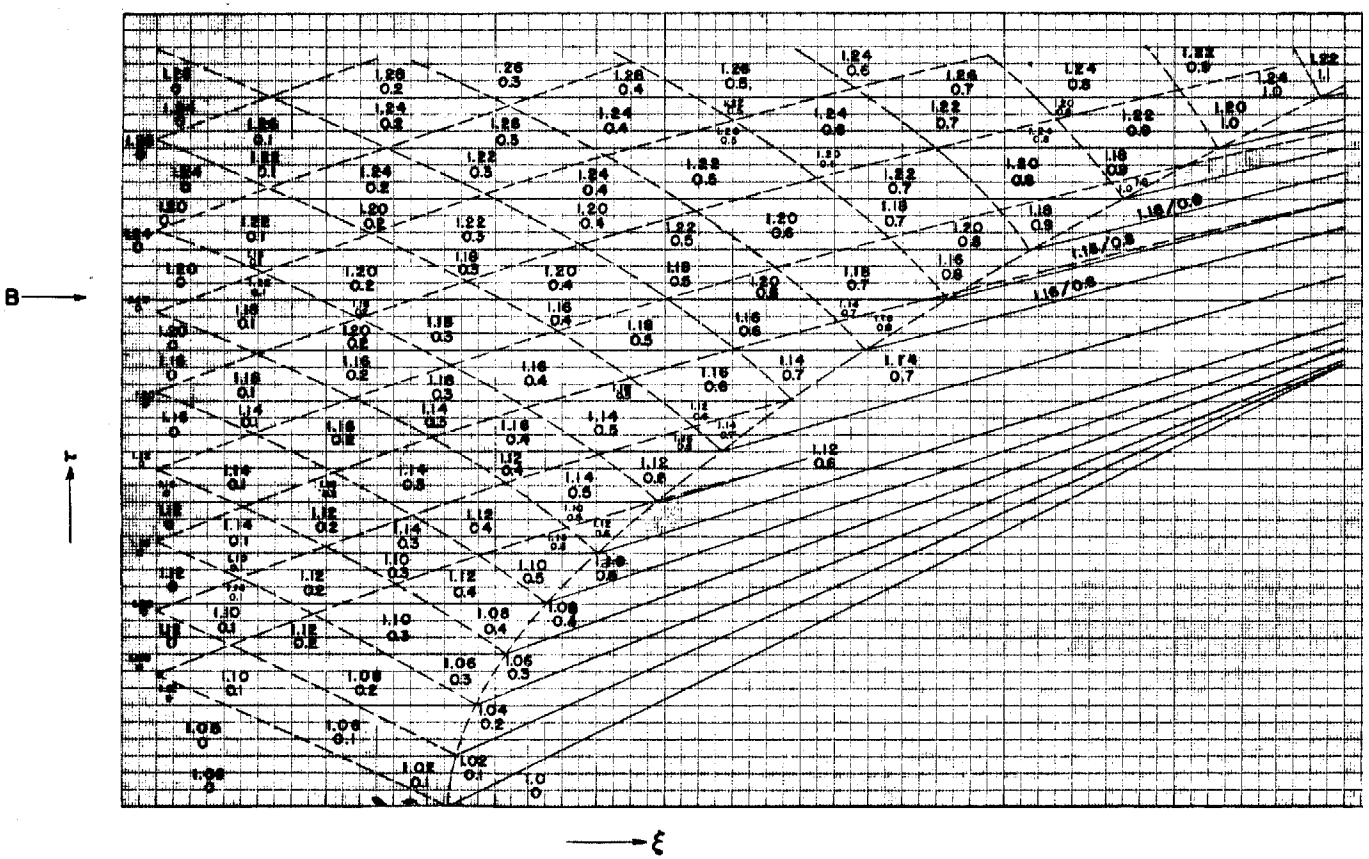

Figure 7'. - Diagram of wave propagation. Combustion. (An 11 1/2-by 15 1/4-in. print of this figure is attached.)

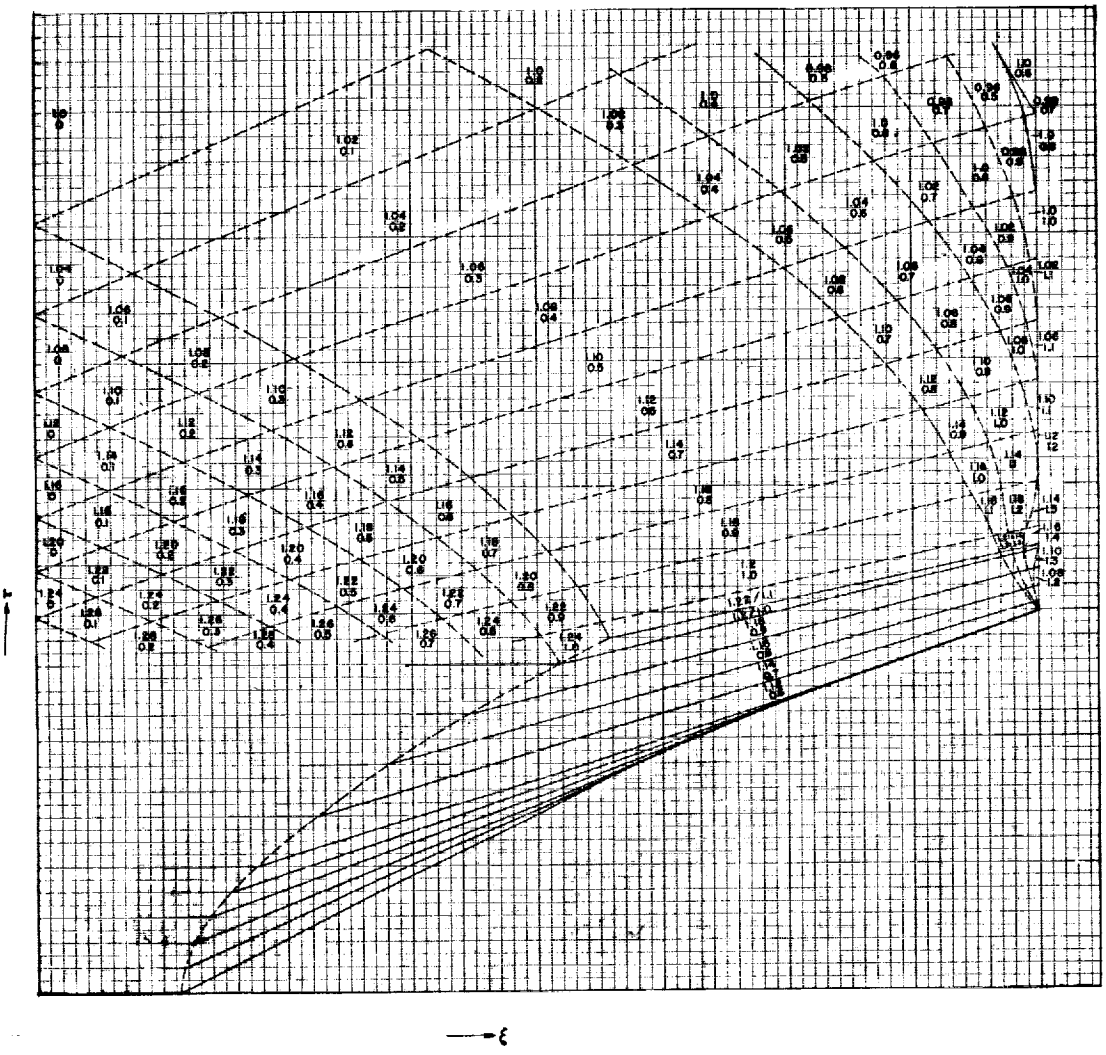

Figure 8'. - Diagram of wave propagation. First working cycle, exhaust. (A 17 $\frac{1}{2}$-by 18-in. print of this figure is attached.)

621

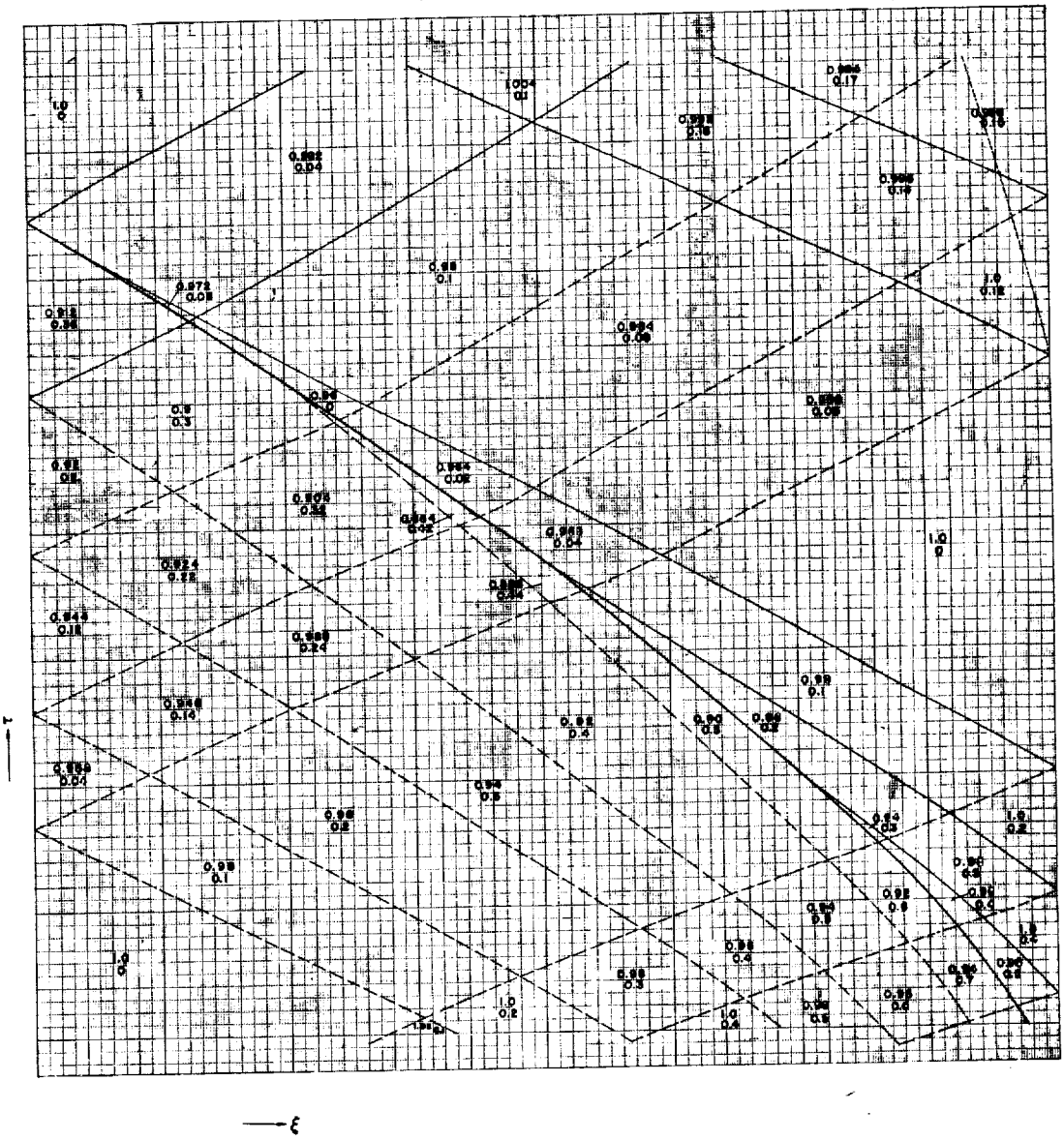

Figure 9'. - Diagram of wave propagation. First working cycle, inlet. (A 16 1/2-by 18-in. print of this figure is attached.)

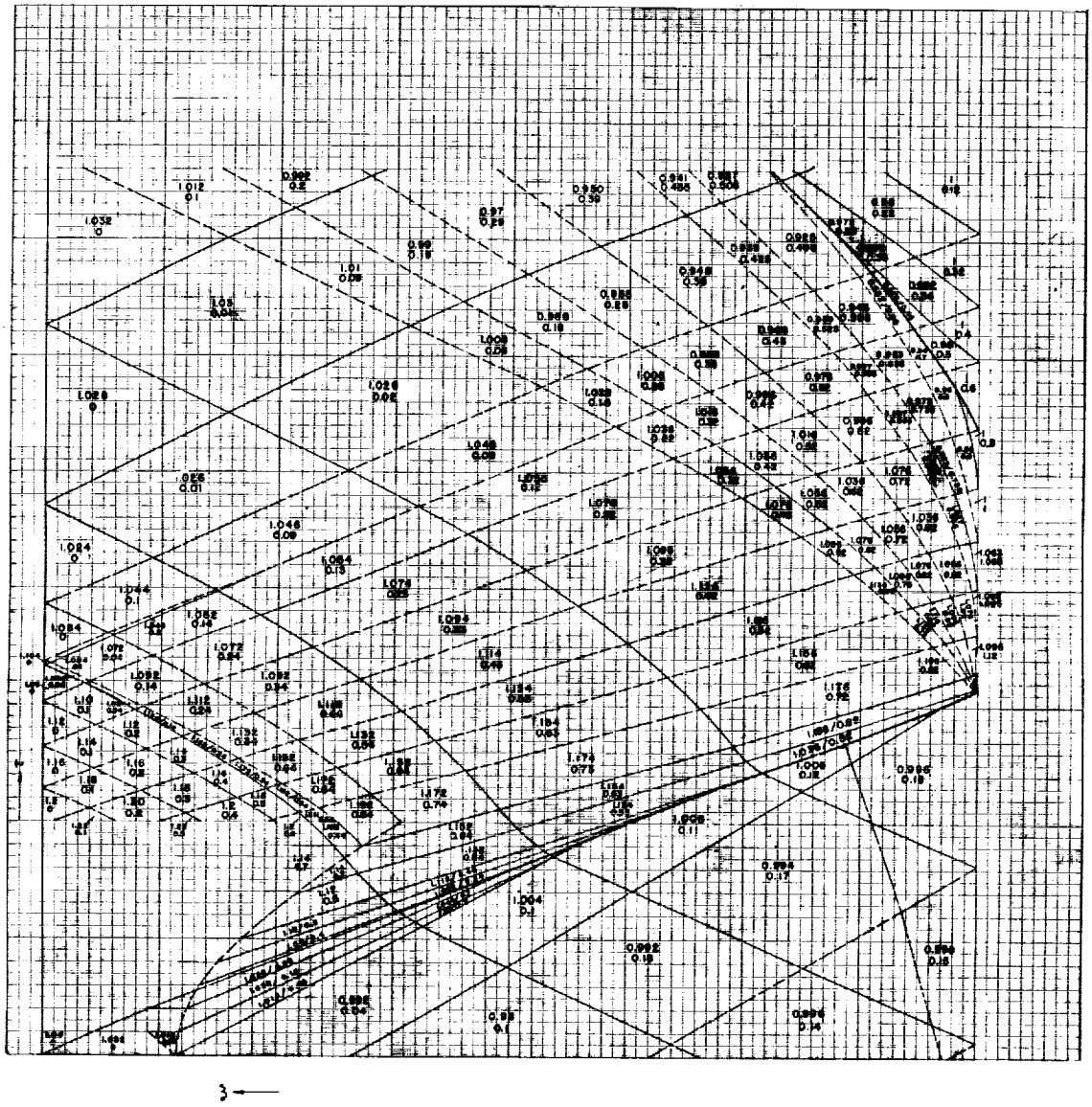

Figure 10'. - Diagram of wave propagation. Second working cycle, exhaust. (A 17 1/2-by 18-in. print of this figure is attached.)

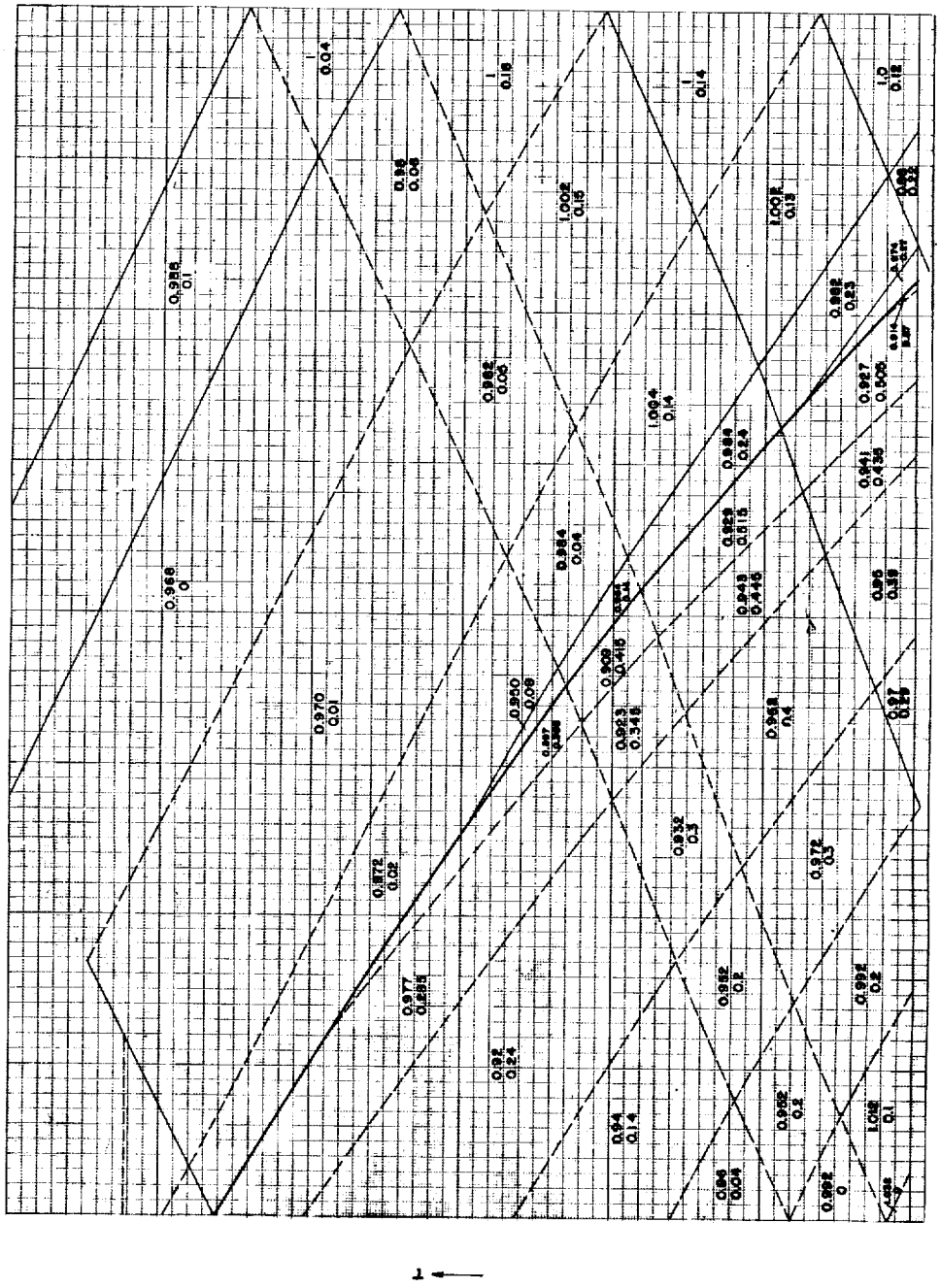

Figure 11'. - Diagram of wave propagation. Second working cycle, inlet. (A $13\frac{1}{2}$- by $16\frac{1}{2}$-in. print of this figure is attached.)